OSAMAH KADHIM HILAL ALMURUMUDHE

ATILIM UNIVERSITY 2021

ANION EXCHANGE MEMBRANE BASED ON SEMIINTERPENETRATING POLYMER NETWORK OF POLYETHER SULFONE / QUATERNIZED STARCH FOR ALKALINE FUEL CELLS

THE GRADUATE SCHOOL OF NATURAL AND APPLIED SCIENCES
OF
ATILIM UNIVERSITY

OSAMAH KADHIM HILAL ALMURUMUDHE

A MASTER OF SCIENCE
THESIS
IN
THE DEPARTMENT OF CHEMICAL ENGINEERING

APRIL 2021

ANION EXCHANGE MEMBRANE BASED ON SEMIINTERPENETRATING POLYMER NETWORK OF POLYETHER SULFONE / QUATERNIZED STARCH FOR ALKALINE FUEL CELLS

A THESIS SUBMITTED TO
THE GRADUATE SCHOOL OF NATURAL AND APPLIED SCIENCES
OF
ATILIM UNIVERSITY

BY

OSAMAH KADHIM HILAL ALMURUMUDHE

IN PARTIAL FULFILLMENT OF THE REQUIREMENTS
FOR
THE DEGREE OF MASTER OF SCIENCE
IN
THE DEPARTMENT OF CHEMICAL ENGINEERING

APRIL 2021

Approval of the Graduate School of Natural and Applied Sciences, Atilim University.

_____

Prof. Dr. Ender Keskinkılıç
Director

I certify that this thesis satisfies all the requirements as a thesis for the degree of Master of Chemical Engineering in the Department of Chemical Engineering Atilim University.

_____

Prof. Dr. Şeniz Özalp Yaman
Head of Department

This is to certify that we have read the thesis ANION EXCHANGE MEMBRANE BASED ON SEMIINTERPENETRATING POLYMER NETWORK OF POLYETHER SULFONE / QUATERNIZED STARCH FOR ALKALINE FUEL CELLS submitted by OSAMAH KADHIM HILAL ALMURUMUDHE and that at in our opinion it is fully adequate, in scope and quality, as a thesis for the degree of Master of Chemical Engineering.

_____ _____

Prof. Dr. Qusay F. Alsalhy
Co-Supervisor

Asst. Prof. Dr. Enver Güler
Supervisor

Examining Committee Members:

Prof. Dr. Nalan Kabay
Chemical Engineering Department, Ege University _____

Asst. Prof. Dr. Enver Güler
Chemical Engineering Department, Atilim University _____

Asst. Prof. Dr. Salih Ertan
Chemical Engineering Department, Atilim University _____

Date: *27/4/2021*

I hereby declare that all information in this document has been obtained and presented in accordance with academic rules and ethical conduct. I also declare that, as required by these rules and conduct, I have fully cited and referenced all material and results that are not original to this work.

Name, Last Name: OSAMAH KADHIM HILAL ALMURUMUDHE

Signature:

ABSTRACT

ANION EXCHANGE MEMBRANE BASED ON SEMIINTERPENETRATING POLYMER NETWORK OF POLYETHER SULFONE / QUATERNIZED STARCH FOR ALKALINE FUEL CELLS

OSAMAH KADHIM HILAL ALMURUMUDHE

M.S., Department of Chemical Engineering

Supervisor: Asst. Prof. Dr. Enver Güler

Co-Supervisor: Prof. Dr. Qusay F. Alsalhy

April 2021, 55 pages

Many effective devices that emerged and developed to generate power without toxic emissions. Proton exchange membrane fuel cell (PEMFC) is one of these effective devices. Its fully dependence on platinum as electrocatalyst has limited its application in a highly competitive market. Potential use of non-precious metal catalyst makes anion exchange membrane fuel cell (AEMFC) garnering renewed attention. Anion exchange membrane (AEM) is considered as the heart of the (AEMFC) and at the same time the preparation as the biggest challenge in the development of (AEMFC). Fabrication of those AEMs with high conductivity and with high alkali resistance has become an active research area for investigation. In this work, two types of anion exchange membranes for alkali fuel cells have been fabricated according to a simple and novel strategy by single step quaternization/crosslinking of starch with choline chloride and epichlorohydrin then blending it with polyethersulfone resulted in a semiinterpenetrating polymer network. The first type, the porous polyether sulfone AEM with 133.33 μm thickness exhibited water uptake of 376.7% and swelling ratio of 5.3%. The second type, the dense polyether sulfone AEM with 55.48 μm exhibited water uptake of 69.9% and swelling ratio of 7.5%

The charaterization results confirmed that our fabrication route was very successful and our fabricated AEMs are very promising candidates for alkaline fuel cell applications.

Keywords: Anion Exchange Membrane, Anion Exchange Membrane Fuel Cell, Dense Polyether Sulfone Anion Exchange Membrane, Porous Polyether Sulfone Anion Exchange Membrane, Semi-interpenetrating Polymer Network.

ÖZ

ALKALİ YAKIT HÜCRELERİ İÇİN YARI-İÇ İÇE GEÇEN POLİETERSÜLFON / KUATERNİZE NİŞASTA POLİMER AĞINA DAYALI ANYON DEĞİŞİM MEMBRANI

OSAMAH KADHIM HILAL ALMURUMUDHE
M.S. Kimya Mühendisliği Bölümü
Tez Yöneticisi : Dr. Öğr. Üyesi Enver Güler
Ortak Tez Yöneticisi : Prof. Dr. Qusay F. Alsalhy

Nisan 2021, 55 sayfa

Zehirli emisyonlar olmadan güç üretmeye yönelik birçok etkili cihaz ortaya çıkmış ve geliştirilmiştir. Proton değişim membranlı yakıt hücresi (PEMFC) bu etkili cihazlardan biridir. Elektrokatalizör olarak platine tamamen bağımlı olması son derece rekabetçi olan pazardaki uygulamasını sınırlandırmıştır. Değerli olmayan metal katalizörün potansiyel kullanımı, anyon değişim membranlı yakıt hücresinin (AEMFC) yeniden dikkati çekmesini sağlamıştır. Anyon değişim membranı (AEM), AEMFC'nin kalbi olarak kabul edilir ve aynı zamanda AEM´lerin hazırlanması, bu yakıt hücrelerin geliştirilmesindeki en büyük zorluk olarak kabul edilmiştir. Yüksek iletkenliğe ve yüksek alkali direncine sahip anyon değişim membranların üretimi, bu alanda aktif bir araştırma alanı haline gelmiştir. Bu çalışmada, alkali yakıt hücreleri için iki tür anyon değişim membranı, basit ve yeni bir stratejiye göre tek aşamalı kuaternizasyon yöntemi ile üretilmiştir, Nişastanin kolin klorür ve epiklorohidrin ile kuaternizasyonu/ çapraz bağlanması ve ardından polietersülfon (PES) ile karıştırılması, iç içe geçen bir polimer ağıyla (IPN) sonuçlanmıştır. Birinci tip, 133.33 µm kalınlığa sahip gözenekli polieter sülfon AEM, % 376.7 su alımı ve % 5.3 şişme

oranı sergilemiştir. İkinci tip ise, 55.48 µm ile yoğun polieter sülfon AEM, % 69.9 su alımı ve % 7.5 şişme oranı sergilemiştir. Karakterizasyon sonuçları, üretim rotamızın çok başarılı olduğunu ve üretilen anyon değiştirici membranlarımızın alkali yakıt hücresi uygulamaları için umut verici olduğunu doğrulamıştır.

Anahtar Kelimeler: Anyon Değişim Membranı, Anyon Değişim Membranlı Yakıt Hücresi, Yoğun Polieter Sülfon Anyon Değişim Membranı, Gözenekli Polieter Sülfon Anyon Değişim Membranı, Yarı-İç İçe Geçen Polimer Ağı.

To my beautiful family, to my mother, my brother, my sister and to my brother's daughters Ruqaya and Fatima.

ACKNOWLEDGEMENTS

My sincere thanks and gratitude to my supervisor Asst. Prof. Dr. Enver Güler to give me the opportunity to work on this important topic. Asst. Prof. Dr. Enver has an amazing personality, like the rest of the Turkish people, he is a kind-hearted and well-mannered person, on the other hand he possesses sharp intelligence and the ability to communicate his ideas to his students, while dealing with him, he makes you feel different wonderful feelings: sometimes you feel that he is a brother, another sometimes you listen to his words as if he is your best friend, but the most important and sweetest feeling when he makes you feel that he is a professor who leads you towards creativity, indeed he is a distinguished and beloved person. Thanks god, I was so lucky to work with such a great professor. Thank you Dr. Enver for your advice, patience and great direction.

My sincere appreciation to my co-supervisor, Prof. Dr. Qusay Alsalhy for his advices. Prof. Dr. Qusay is one of the best professors of Iraq in the field of membrane technology, his leadership personality and spirit of cooperation make working with him easy and enjoyable at the same time, we faced many obstacles but his wise and smart advices always made us overcome these obstacles, working with such a great professor made me gain a lot of experience and also a lot of ideas for the future. God willing, in the future I would be happy to work again with Prof. Dr. Qusay on another great idea and another great research.

I would like to thank my wonderful colleague Ezgi Karakoç for all her help and support. I thank her for the help in translating the abstract into Turkish language. She has a compassionate soul and a heart full of love, thank you Ezgi and I wish you a life full of happiness and success.

My sincere thanks to my family for their support and for their encouragement throughout my graduate study. Their prayers and love are the ones that have given me the strength to make this dream come true.

TABLE OF CONTENTS

LIST OF TABLES

TABLES

LIST OF FIGURES

FIGURES

LIST OF SYMBOLS/ABBREVIATIONS

AEM	Anion Exchange Membrane
AEMFC	Anion Exchange Membrane Fuel Cell
AFC	Alkaline Fuel Cell
BCMB	1,4-Bis (Chloro Methoxy) Butane
BPPO	Brominated Poly (2,6-Dimethyl-1,4-Phenylene Oxide)
C	Carbon
CC	Choline Chloride
Cl	Chlorine
CM-PAEK	Chloromethylated Poly (Arylene Ether Ketone)
CMPSF	Chloro Methylated Poly sulfone
DABCO	1,4 - Diazabicyclo [2.2.2] - Octane
DMSO	Di Methyl sulfoxider
ECH	Epichlorohydrin
ETFE	Ethylene Tetra Fluoro Ethylene
FEP	Fluorinated Ethylene Propylene
FTIR	Fourier Transform Infrared
IEC	Ion Exchange Capacity
IPN	Interpenetrating Polymer Network
ISP	Ion-Solvating Polymer
KOH	Potassium Hydroxide
MCFC	Molten Carbonate Fuel Cell
Na	Sodium
O	Oxygen
PAA	Poly (Acrylic Acid)
PAFC	Phosphoric Acid Fuel Cell
PBI	Polybenzimidazole
PEEK	Poly (Ether Ether Ketone)
PEMFC	Proton Exchange Membrane Fuel Cell

PEO	Poly Ethylene Oxide
PES	Poly Ether Sulfone
Poly (VBC-co-ɣ-MPS)	Poly (Vinylbenzyl Chloride-c--ɣ-Methacryloxy Propyl Trimethoxy Silane)
PPO	Poly (Phenylene Oxide)
PSEBS	Poly (Styrene – Ethylene / Butylene - Styrene)
PSU	Poly Sulfone
PVA	Poly Vinyl Alcohol
PVP	Poly (Vinyl Pyrrolidone)
QAPEK-OH	Quaternary Ammonium Polyether Ketone Hydroxide
QPS	Quaternized Poly Sulfone
rGO	Reduced Graphene Oxide
S	Sulfur
SEBS	Poly Styrene – block –Poly (Ethylene –ranbutylene)-block - Styrene
SEM	Scanning Electron Microscopy
Semi-IPN	Semi-Interpenetrating Polymer Network
SOFC	Solid Oxide Fuel Cell
SR	Swelling Ratio
ST	Starch
TMEDA	Trimethyl Butylene Di Amine
UV	Ultra Violet
VBC	Vinyl Benzyl Chloride
WU	Water Uptake
γ-MPS	γ-Methacryloxy Propyl Trimethoxy Silane

CHAPTER 1

INTRODUCTION

1.1 Fuel Cells

Significant and rapid growth of global population, as well as significant and rapid industrial development require massive energy supply to meet their needs, consequently relying only on the conventional energy sources to secure this huge amount of supply will contribute greatly to the exacerbation of the pollution crisis in our world [1]. From this perspective searching alternative sources of energy generation to meet these massive needs and also to handling or at least mitigating the problem of environmental pollution have gained significant importance [2]. Indeed over the last few decades several alternative energy technologies have emerged and developed, of course, fuel cell technology was one of these technologies [3]. Fuel cells as shown in Figure 1.1 are devices that produce electrical energy without toxic emissions efficiently by exploiting the chemical energy stored in the fuels bonds. thus, it is considered as the most unique one among these alternatives [4].

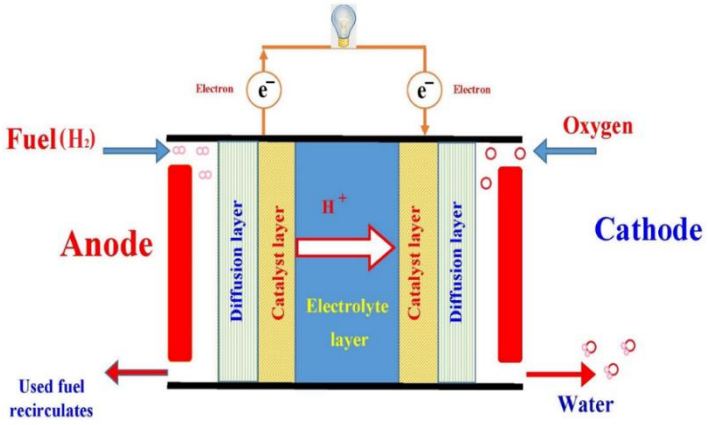

Figure 1.1 Single hydrogen fuel cell parts.

Hence, intensive efforts of scientists and researchers have greatly contributed to develop the fuel cell technology and strengthening it is existence in our life [5]. Fuel cells are divided into various types [6]. The most common types are alkaline fuel cell (AFC), phosphoric acid fuel cell (PAFC), molten carbonate fuel cell (MCFC), solid oxide fuel cell (SOFC), and polymeric electrolyte membrane fuel cell (PEMFC) [7]. Owing to its attractive properties, low temperature operation and high power density the polymeric electrolyte fuel cell is considered the best one [8]. Based on the type of polymer electrolyte membrane, the polymeric electrolyte membrane fuel cell divided into two types [9]. The first is the proton exchange membrane fuel cell and the second is the anion exchange membrane fuel cell [10]. Owing to its low operating temperature and quick start-up the proton exchange membrane fuel cell PEMFC has received attention [11]. High cost fabrication of PEMFC due to the dependence on noble metal catalysts hampered its widespread commercialization [12]. Actually, anion exchange membrane fuel cell (AEMFC) as shown in Figure 1-2 is just an immitation to the (PEMFC) [13].

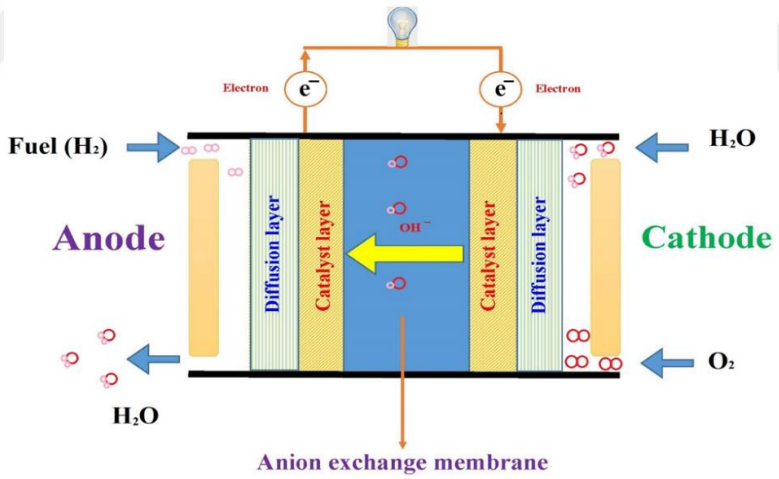

Figure 1.2 Anion exchange membrane fuel cell.

But in the AEMFC the PEM is replacing with AEM allows hydroxide ion to pass through it from the cathode to the anode while blocking the proton [14]. Hence, it is considered as viable alternative to the (PEMFC) [15]. The potential use of non-precious metal catalyst makes AEMFC attractive, but before the practical application

and commercialization, AEMs with high alkali stability and with high hydroxide conductivity should be developed [16]. In AEMFC device the AEM is the key differentiating element conducts hydroxide ions from the cathode to the anode [17]. The anodic, cathodic and overall reaction of AEMFC are [18]:

$$H_2 + 2OH^- \rightarrow 2H_2O + 2e^- \quad (1)$$

$$\frac{1}{2} O_2 + H_2O + 2e^- \rightarrow 2OH^- \quad (2)$$

$$H_2 + \frac{1}{2} O_2 \rightarrow H_2O \quad (3)$$

1.2 Alkaline fuel cells (AFC)

AFC using aqueous KOH as electrolyte was the first practical type of fuel cells [19]. NASA in the middle of the last century used this technology for its space applications. This type of fuel cell got a lot of attention at first, but then it faced many problems which contributed to reduce interest in it [19]. Interest in AFCs have created again in virtue of the scientific advance related to (PEMFC) [20]. The previous problems had been solved by using a solid polymer membrane as an electrolyte [20]. The expectations of researchers and scientists all confirm that in the near future the alkaline polymer electrolyte fuel cell will be used in massive power applications [20].

1.3 Membranes for AFC applications

Many polymers are used and huge number of AEMs have been fabricated for many applications and certainly the alkaline fuel cell is one of the most important of these applications [21]. Fabrication of AEMs needs performing chloromethylation and quaternization reactions which in turn lead to many health risks, Hence, strenuous efforts made by the researchers and scientists to reach facil fabrication approaches with minimizes health risks [22]. AEMs for AFC applications are classified into three types : heterogeneous, IPN, and homogeneous AEMs.

1.3.1 Heterogeneous AEMs

The efforts aimed at fabrication AEMs with comparable performance to homogeneous one led to produce heterogeneous AEMs [23]. These AEMs possess good mechanical strength, on the other hand these AEMs have lower conductivity and selectivity [24]. The heterogeneous AEMs are divided into two types ion solvating polymer and hybrid membrane.

1.3.1.1 Ion solvating polymer (ISP)

These AEMs are composed from ternary system polymer/ KOH / water, the most developed system is based on polyethylene oxide in virtue of its ability to coordinate with metal ions which eventually resulting in homogeneous polymer films. The ionic conductivity is strongly dependent on the amounts of KOH and water in the films. Fauvarque et al. [25] developed a class of ISPs, based on PEO, KOH, and optionally, water. Salmon et al. [26] synthesized ISPs based on poly (ethylene oxide) (PEO), the ionic conductivity of the developed ISPs reached 1 mS/cm at room temperature. On the other way, a lot of researchers exploited the easy preparation and biodegradability of poly (vinyl alcohol) (PVA). Dragana et al. [27] synthesized ISPs based on poly (vinyl alcohol) (PVA) the developed ISPs reached ionic conductivity of 12 mS/cm at 25 ℃. Uday and Hiralal [28] developed ISPs based on poly (vinyl alcohol) and used it for alkaline fuel cell applications, the fabricated membrane showed good properties and the performance of single cell confirmed that the developed ISPs could be used as a suitable solid electrolyte for alkaline fuel cell applications. A few researchers attempted to exploit polybenzimidazole PBI to develop ISPs for alkaline fuel cell applications [29]. Xing and Savadogo [30] synthesized ISPs based on polybenzimidazol PBI and used it for alkaline fuel cell applications, the fabricated membrane reached ionic conductivity up to 10 mS/cm at 90 ℃. Hadis et al. [31] were had a new vision for the topic, they synthesized novel KOH-doped porous polymeric membrane for alkaline fuel cell applications, the developed ISPs reached ionic conductivity of 49 mS/cm at room temperature. Wu et al. [32] used a free radical polymerization and solution casting method to develop ISPs based on poly vinyl alcohol (PVA)/ poly (acrylic acid) (PAA) blend, the developed ISPs reached ionic conductivity of 301 mS/cm, also the fabricated ISPs showed a very good thermal and

mechanical properties. Jing et al. [33] developed unique ISPs based on poly (vinyl alcohol) (PVA)/ poly (vinylpyrrolidone) (PVP) blend, the synthesized ISPs showed a very good properties and reached ionic conductivity of 53 mS/cm at room temperature.

1.3.1.2 Hybrid AEMs

The desired characteristics of polymers and the desired characteristics of inorganic supplements are combined together to form the hybrid membranes [34]. The usual preparation method is the sol-gel method [35]. But also several methods beside sol-gel are possible. Ying et al. [36] synthesized series of hybrid AEMs through sol-gel process based on poly (vinyl alcohol) (PVA) with different ratios of silica and used it for alkaline fuel cell applications, the fabricated hybrid membranes showed ionic conductivity of 14 mS/cm at 60 ℃. Liang et al. [37] prepared hybrid anion membrane based on chloromethylated polysulfone (CMPSF) and functionalized polyhedral oligomeric silsesquioxane (POSS), the synthesized anion membrane showed (water uptake 45.20% at 80 ℃), (swelling ratio 22.28% at 80℃) and ionic conductivity of 6.84 mS/cm at 80 ℃. Feng et al. [38] developed a series of imidazolium-based hybrid anion exchange membranes for alkaline fuel cell applications, the fabricated hybrid AEMs reached ionic conductivity of 10 mS/cm at room temperature. Zhu et al. [39] fabricated promising hybrid AEMs for alkaline fuel cell applications, they used the quaternized polysulfone (QPS) and functionalized titanium dioxide to obtain the hybrid anion exchange membranes, the fabricated hybrid AEMs reached ionic conductivity of 31 mS/cm and showed acceptable alkaline stability. Ji et al. [40] developed hybrid anion exchange membrane by introducing reduced graphene oxide (rGO) into chloromethylated poly (arylene ether ketone) (CM-PAEK) and used it for alkaline fuel cell applications, the fabricated hybrid anion exchange membrane reached ionic conductivity of 115 mS/cm. Wu et al. [41] synthesized series of hybrid anion exchange membrane and used it for alkaline fuel cell applications, they were used quaternized vinylbenzyl chloride (VBC) and γ-methacryloxypropyl trimethoxy silane (γ-MPS) to obtain the hybrid anion exchange membrane, the fabricated membranes reached ionic conductivity up to 0.4 mS/cm. Lin et al. [42] used brominated poly (2,6-dimethyl-1,4-phenylene oxide) (BPPO) with poly (vinylbenzyl chloride-co-ɣ-methacryloxypropyl trimethoxy silane) (poly(VBC-co-ɣ-MPS) to

fabricate hybrid AEMs for alkaline fuel cell applications, the developed hybrid AEMs reached ion exchange capacity of 2.27 mmol/g^{-1} and reached ionic conductivity up to 12 mS/cm.

1.3.2 Interpenetrating polymer network (IPN)

IPN materials have drawn a great interests in virtue of the special properties brought about by the interlocking of polymer chains. IPN is a combination of hydrophobic polymer that has a good thermal, chemical and mechanical properties, and a conductive polymer, one at least is synthesized and / or cross / linked in the immediate presence of the other without any covalent bonds between them [43]. Jiandang et al. [44] used quaternized polystyrene and crosslinked poly (2,6-dimethyl-1,4-phenylene oxide) to construct s-IPN based anion exchange membrane and used it for alkkaline fuel cell applications, the developed s-IPN showed low swelling ratio of 12% and reached an ion exchange capacity of 1.44 meq.g^{-1}, ionic conductivity of 37.2 mS/cm at 20 ℃. Weihong et al. [45] developed s-IPN of poly (phenylene oxide) and poly (Vinyl alcohol) and used it for alkaline fuel cell applications, the developed s-IPN reached an ion exchange capacity of 1.46 mmol/g and displayed very good ionic conductivity at 60 ℃. Lingping et al. [46] constructed fully IPN and used it for alkaline fuel cell applications, the constructed IPN showed water uptake of 67.5%, swelling ratio of 11% and it reached an ion exchange capacity of 1.75 mmol/g^{-1}, ionic conductivity of 257.8 mS/cm at 80 ℃. Zeng et al. [47] constructed fully IPN using blend of poly (vinyl alcohol) and poly (vinylbenzyl chloride) and used it for alkaline fuel cell applications, the constructed IPN reached an ion exchange capacity of 1.61 mmol/g^{-1} and showed ionic conductivity of 141.7 mS/cm at 80 ℃. Sydonne et al. [48] developed novel semi-IPN for fuel cell applications, mixture of polysulfone (PSU) functionalized with 1-methylimidazolium and crosslinked with TMEDA and sulfonated polysulfone, The developed anion membrane (100 µm) showed water uptake of 25% and ionic conductivity of 11 mS/cm at room temperature.

1.3.3 Homogeneous membranes

Strenuous efforts made by the researchers and scientists on the synthesis of homogeneous AEMs with good stability and with high conductivity . Homogeneous

AEMs obtained according to a hazardous and complicated procedures which require chloromethylation and then quaternization to create quaternary ammonium head group tethered to an aromatic ring through a benzyl linkage [49].

1.3.3.1 Polymerization or polycondensation of monomers containing cationic characters

The (co)polymerization and quaternization of chloromethylstyrene represents a very easy procedure to fabricate homogeneous AEM. Sata and colleagues [50] synthesized two series of homogeneous AEMs using poly(styrene)-based copolymer with low and high divinyl benzene as a cross-linking agent, the obtained an ion exchange capacity was a good value around 0.00238 eq/g. Iravaninia and Rowshanzamir [51] fabricated homogeneous AEMs using quaternized polysulfone with ammoium cation moieties and used it for alkaline fuel cell applications, the developed anion exchange membranes reached an ion exchange capacity of 1.73 meq/g and showed ionic conductivity of 34.01 mS/cm at 80 ℃. Tomoi et al. [52] fabricated homogeneous AEM using bromoalkoxy styrenes and bromoalkoxy methyl styrenes, and DVB to cross-link quaternized polymers followed by quaternization with triethylamine. This homogeneous AEM reached an ion exchange capacity of 0.004 eq/g. Ge et al. [53] developed anion exchange membrane by the quaternization of the hyperbranched poly(4-vinylbenzyl chloride) (HB-PVBC) with a multiamine oligomer poly(N,N-Dimethylbenzylamine), the prepared membrane exhibited 47% water uptake, 12.3% swelling ratio and 33 mS/cm at room temperature. Sayema et al. [54] synthesized homogeneous anion exchange membrane using polystyrene copolymers crosslinked with dialkyne via click reaction, the fabricated AEMs reached an ion exchange capacity of 2.04 meq/g and showed ionic conductivity of 21 mS/cm. Qing et al. [55] developed homogeneous AEMs for alkaline fuel cell applications, they were used polystyrene-block-poly(ethylene-ranbutylene)-block-polystyrene (SEBS) to prepare the anion exchange membranes, the fabricated AEMs reached ionic conductivity of 9.37 mS/cm at 80 ℃. Taro et al. [56] developed homogeneous anion exchange membranes for alkaline fuel cell applications, the developed AEMs containing hexafluoroisopropylidene groups as the hydrophobic component and fluorenyl groups substituted with pendant hexyltrimethylammonium groups as the hydrophilic

component, this unique homogeneous membrane reached ionic conductivity of 134 mS/cm at 80 ℃. Luo et al. [57] fabricated a quaternized poly(methylmethacrylate-co-butyl-acrylate-co-vinylbenzyl), using methyl methacrylate, vinyl benzyl chloride, and butyl acrylate. Valade et al. [58] synthesized homogeneous AEMs by cationization of polymers, followed by radical polymerization of fluorinated olefins with vinyl ethers.

1.3.3.2 Introduction of cationic characters on a performed film

Monomer modification or grafting of functionalized monomer on the performed film represent a facile way to fabricate homogeneous AEM. Graft copolymerization of monomers onto polymer films was performed via plasma, UV and irradiation.. Varcoe and Slade [59] via radiation-induced grafted polymeization of CMS onto FEP and ETFE, fabricated homogeneous AEM. Quaternary ammonium-functionalized radiation-grafted ETFE was another strategy to fabricate homogeneous AEM with ionic conductivity of 34 mS/cm at 50 ℃. Radiation-grafted trifluorostyrene onto PVDF, PE, ETFE, and PTFE also used to produce some membranes [60]. Amination and cross-linking to the grafted polymer also used to fabricate homogeneous AEM [61]. Plasma polymerization was used to synthesize a cross-linked AEMs for use as an electrolyte in AFCs [62]. The plasma polymerizationhighly led to obtain homogeneous AEM highly cross-linked, uniformly thin, and with good ionic conductivity which around 54 mS/cm [63].

1.3.3.3 Introduction of cationic moieties by chemical modification into a polymer

Massive efforts have been exerted to fabricate homogeneous AEM by chemical modification. Dragan and colleagues [64] fabricated homogeneous AEMs by chemical modification, they used chloromethylmethyl ether in their work. Vinodh et al. [65] through chloromethylation and quaternization of a (PSEBS) by the triethylamine, they used hydrochloric acid instead of chloromethyl methyl ether. Stability of aliphatic polyethers in alkaline medium made Agel and colleagues [66] used DABCO with polyether based on epichlorohydrin to fabricate their AEM. Stoica et al. [67] fabricated their AEM using poly(epichlorohydrin) copolymer with allyl glycidyl ether as cross-linking agent, DABCO and 1-azabicyclo-[2.2.2]-octane (quinuclidine). By the

reaction between chlorinated polypropylene and ethylene diamine a new AEMs were recently fabricated [68]. Xiong et al. [69] used glutaraldehyde as crosslinker and grafted quaternary ammonium groups on the PVA backbone using (2,3-epoxypropyl) trimethylammonium chloride AEMs based on PVA, their AEMs reached ionic conductivity of 7 mS/cm at room temperature. The using of 1,4-bis (chloromethoxy) butane (BCMB) as chloromethylating reagent for poly (phthalazinone ether sulfone ketone) (PPESK), poly (ether ether ketone) (PEEK), and poly (ether sulfone) (PES) was a successful strategy to avoid the carcinogenic chemicals and obtain the anion exchange membrane, the synthesized AEMs showed good ionic conductivity, good ion exchange capacity and good chemical stability [70]. The chloromethylation of polysulfone followed by quaternization was another strategy to prepare the anion exchange membrane for alkaline fuel cell applications, the obtained membranes by using this strategy exhibited good ionic conductivity but poor mechanical strength and high swelling ratio [71]. Iravaninia et. al. [72] via chloromethylation, amination and alkalization of polysulfone (QAPSFs) synthesized series of homogeneous AEMs , the fabricated AEMs reached ion exchange capacity of 1.43 meq/gr and ionic conductivity of 26.32 mS/cm at 80 ℃. Gopi et. Al. [73] via the chloromethylation of poly(phenylene oxide) (PPO) by aryl substitution then followed by quaternization fabricated homogeneous anion exchange membrane, the fabricated AEMs reached ionic conductivity of 8.3 mS/cm at 70 ℃ and ion exchange capacity of 0.70 mmol/g. Zijun et al. [74] used polybenzimidazoles with pendant quaternary ammonium groups as potential anion exchange membranes for fuel cells, the fabricated AEM reached ionic conductivity of 56 mS/cm. Zarrin et al. [75] fabricated series of highly durable quaternary ammonium polyetherketone hydroxide (QAPEK-OH) anion exchange membranes for alkaline fuel cell applications, the fabricated AEMs reached ionic conductivity of 11 mS/cm at 100 ℃. Iravaninia and Rowshanzamir [76] fabricated homogeneous anion exchange membrane with ion exchange capacity of 1.73 meq/gr and with ionic conductivity of 15.87-34.01 mS/cm at 25-80 ℃ was fabricated via chloromethylation, amination and alkalization of polysulfone. Varcoe et al. [77] via chloromethylation, quaternization and hydrolytic reaction synthesized polyether sulfone Cardo AEMs with an ion exchange capacity of 0.00125 eq/g and ionic conductivity of 41 mS/cm. Xi et al. [78] fabricated homogeneous AEM with ionic

conductivity of 140 mS/ cm via introduction of chloromethyl groups and subsequently quaternary ammonium groups into poly(phtalazinone ether sulfone) (PPESK). Liang and coworkers [79] via blending of 30-40 wt% chloroacetylated-PPO with bromomethylated-PPO, fabricated homogeneous AEM with ionic conductivity of 32 mS/cm at 25 ℃.

1.4 Objective of the Thesis

This thesis deals with the adobting of a novel, easy strategy to fabricate suitable anion exchange membrane for alkaline fuel cell applications, and at the same time the fabrication strategy avoided the use of any hazardous chemicals. Such research if achieved by a large percentage on the ground, will certainly be considered as a great contribution to the scientific research aimed at the development of anion exchange membrane fuel cell (AEMFC) and make it valid for the practical application and commercialization. The fabrication of AEMs most of the time requires complicated procedure and dealing with toxic chemicals, hence, in this work we have focused on overcoming this obstacle. The obtained AEMs in this work were fabricated according to easy procedure and with environmentally benign chemicals

CHAPTER 2

EXPERIMENTAL

2.1 Materials

Polyether sulfone (Radel R-5000 with 50 kDa average and 1.28 specific gravity) was purchased from Solvay polymers (Brussels, Belgium), potato starch [$(C_6H_6O_5)_n$ M.W.= $(162.14)_n$] was purchased from HIMEDIA, choline chloride extra pure 99% ($C_5H_{14}ClNO$ M.W.= 139.63 g/mol) was purchased from HIMEDIA, epichlorohydrin (C_3H_5ClO M.W.= 92.53 g/mol, density= 1.18 g/cm^3) was purchased from Scharlau, dimethyl sulfoxide (C_2H_6OS M.W.= 78.13, density= 1.10 g/cm^3) was purchased from CHEM-SUPPLY, NaOH [pellets, (assay ≥ 97%), water soluble 1260 g/L at 20 °C] was purchased from Sigma-Aldrich company.

2.2 Reaction Scheme

The hydroxyl group of the starch is etherified as shown in Figure 2.1 the epoxy ring (originating from epichlorohydrin) is connected to the starch molecule via ether bond. The crosslinking occurred when the epoxy ring reacted with a new molecule of starch as shown in Figure 2.2 Protonation happened to the oxygen atom of the epoxy ring, epoxy ring opened and converted into hydroxypropyl attached between the starch molecules. As shown in Figure 2.2 also epichlorohydrin via hydroxypropyl group connected quaternary ammonium head group (originating from choline chloride) to the starch molecule. By this we obtained the quaternized/crosslinked starch, the final step is so easy, included the blending of quaternized/crosslinked starch with polyethersulfone to form semi-IPN.

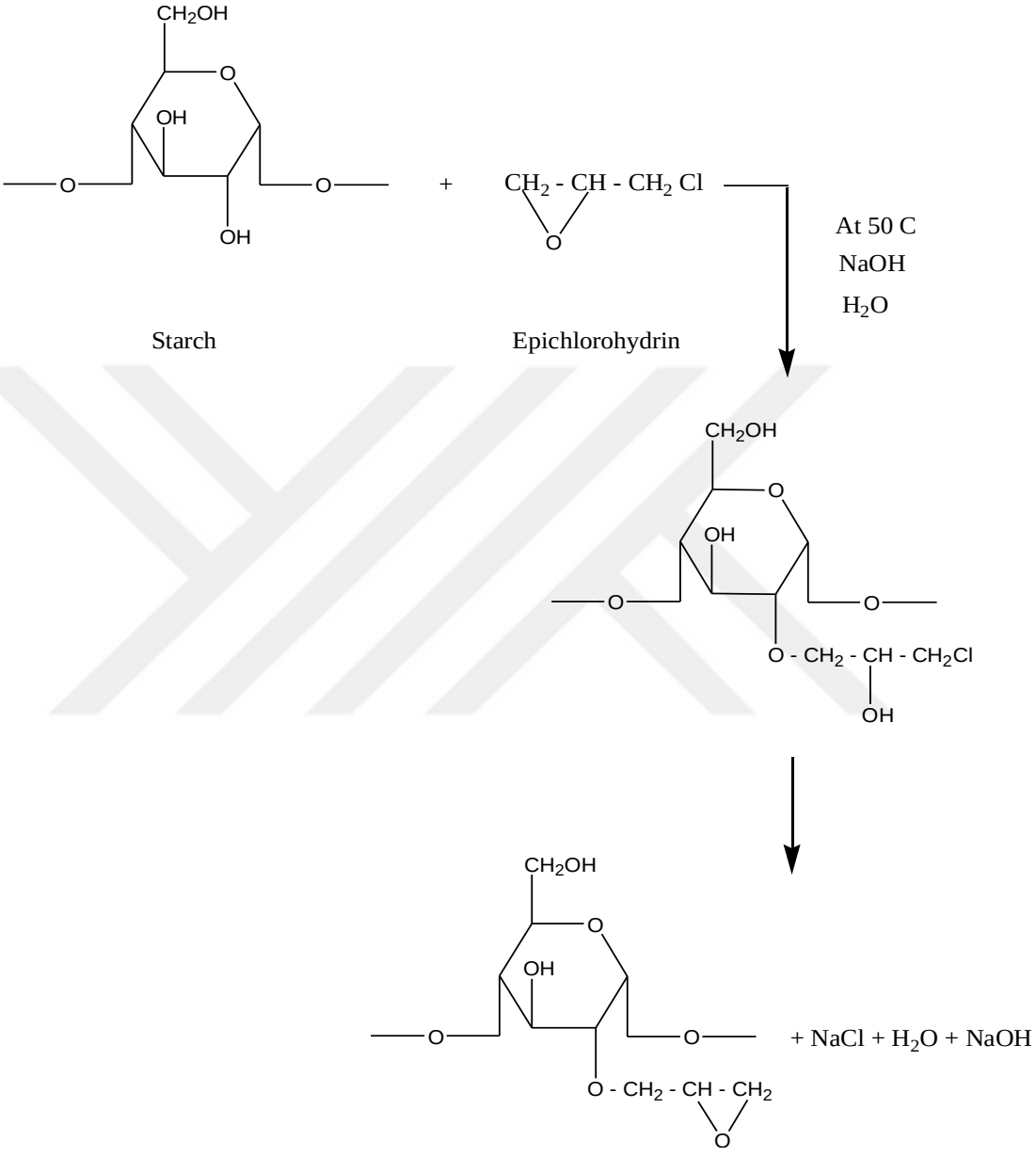

Figure 2.1 Reaction mechanism between starch and epichlorohydrin.

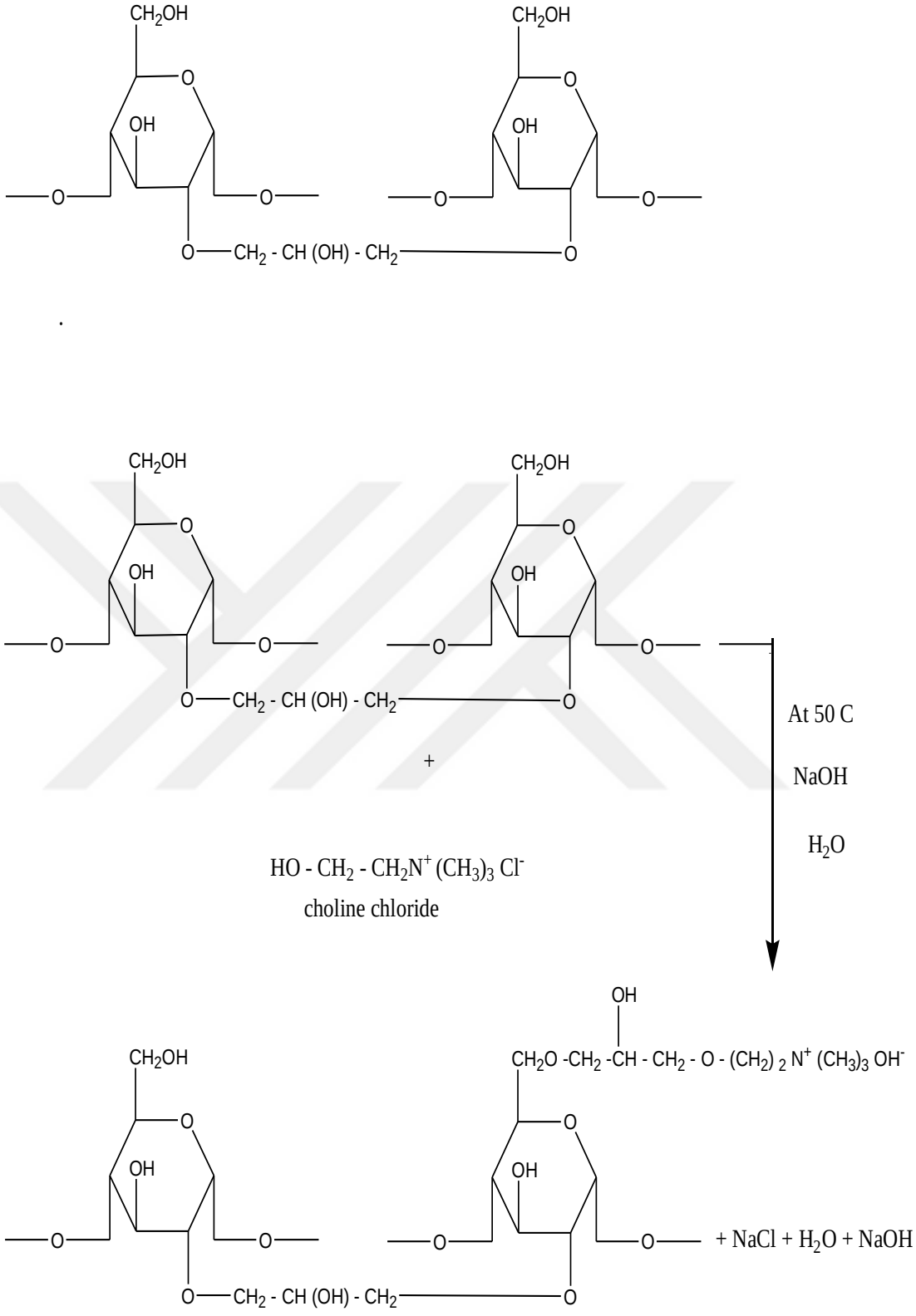

Figure 2.2 Crosslinking and quaternization of starch mechanism.

2.3 Membrane Preparation

The conventional membrane for alkaline fuel cell applications is the dense membrane, but most of the times the ion diffusivity across the dense membrane is low because of its less free volume. Add porosity will increase large free volume and definitely will contribute to increase the ion diffusivity. Here, in this work we fabricated both types porous and dense polyether sulfone AEMs.

2.3.1 Porous polyether sulfone anion exchange membrane

Water uptake is important factor that influences the ion exchange capacity. Hamid et al. [80] developed porous polyether sulfone cation membrane can be used for fuel cell applications, this porous cation membrane was synthesized via wet phase inversion method. In this thesis we fabricated porous polyether sulfone anion exchange membrane via wet phase inversion method.

2.3.1.1 Porous membrane preparation

Starch was dissolved in dimethyl sulfoxide (DMSO) on a magnetic stirrer at 50℃ for (15 min) to obtain solutions of (3.509, 6.78, 9.84, 12.7 wt% starch). Aqueous solution of (1.25 M NaOH) was added to the solution of starch on a magnetic stirrer at 50℃ for 1 h. Single step quaternization/crosslinking of the starch was performed by the adding of 0.2 g choline chloride, 0.2 ml epichlorohydrin on a magnetic stirrer at 50℃ for 5 h. At the same time polyether sulfone was dissolved in DMSO on a magnetic stirrer at temperture 50℃ to obtain 15 wt% polyether sulfone. After that the synthesized quaternized/crosslinked starch added to the polyether sulfone solution on a magnetic stirrer at temperature 50℃ to obtain dope solution with (12.773, 13.23, 13.682, 14.13 total polymer wt%). The dope solution was poured on a glass flat plate. Manual casting (knife thickness = 250 µm) as shown in Figure 2.3 was used to fabricate the membrane.

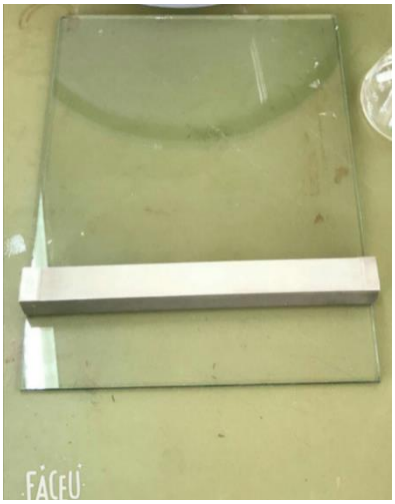

Fıgure 2.3 Manual casting of the membrane.

After casting, the membrane immersed immediately in the coagulation bath of distilled water for 24 h (to ensure complete removal of the solvent), then dried at ambient temperature and kept for characterization tests. In Figure 2.4 schematic diagram of the membrane preparation is shown.

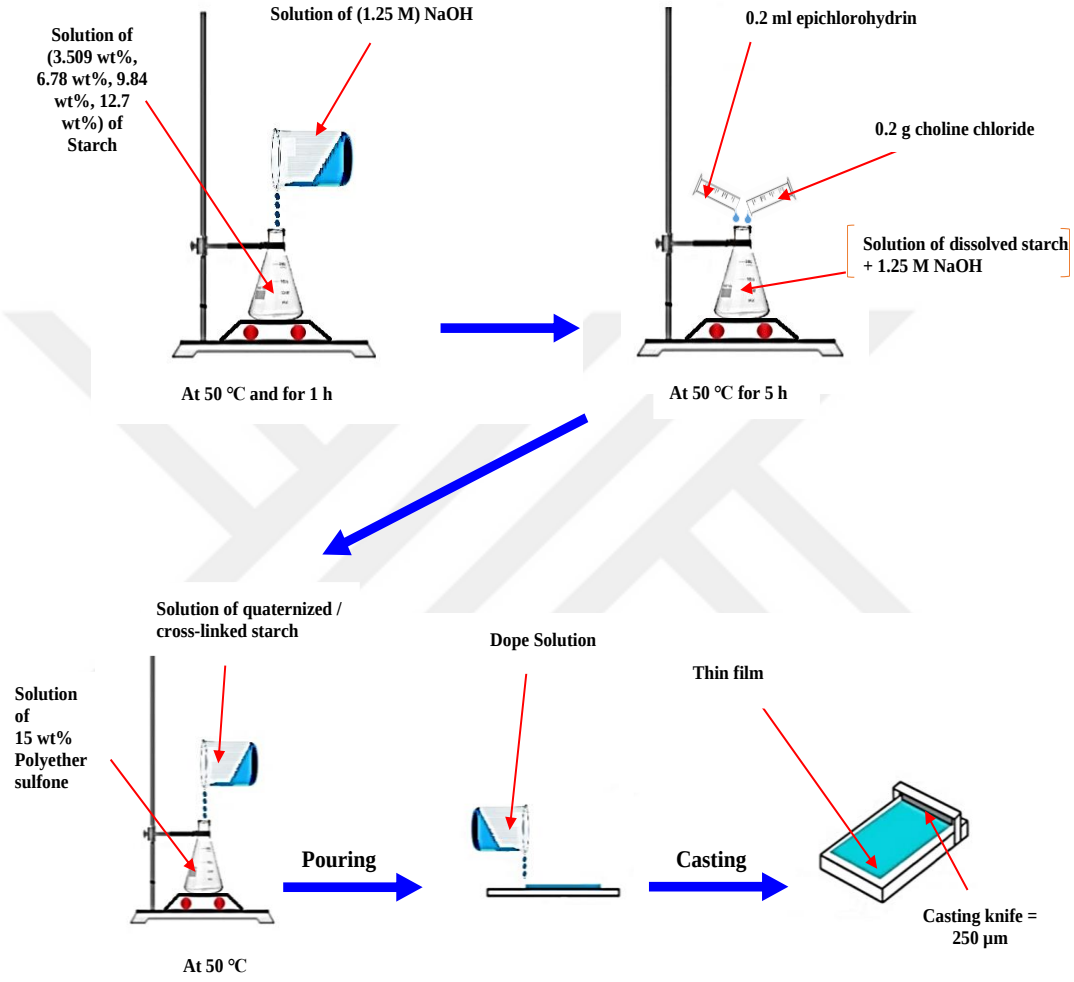

Figure 2.4 Schematic diagram of the porous membrane preparation.

2.3.2 Dense polyether sulfone anion exchange membrane

Dense membrane considered as the conventional type for fuel cell applications. In this thesis we fabricated dense polyether sulfone anion membrane via dry phase inversion method.

2.3.2.1 Dense membrane preparation

Starch was dissolved in dimethyl sulfoxide (DMSO) on a magnetic stirrer at 50 ℃ for 15 min to obtain solution of (3.509, 6.78, 9.84, 12.7 wt% starch), aqueous solution of 1.25 M NaOH was added to the solution of starch on a magnetic stirrer at 50 ℃ for 1 h. Single step quaternization/ crosslinking of the starch was performed by the adding of 0.2 g choline chloride and 0.2 ml epichlorohydrin on a magnetic stirrer at 50℃ for 5 h. At the same time polyether sulfone was dissolved in DMSO on a magnetic stirrer at 50℃ to obtain 15 wt% polyether sulfone. After that the synthesized quaternized/ crosslinked starch added to the polyether sulfone solution on a magnetic stirrer at temperature 50 ℃ to obtain dope solution with (12.773, 13.23, 13.682, 14.13 total polymer wt%). The dope solution was poured on a glass flat plate. Casting mashine (Lab Automatic Wire Bar Coater, knife thickness = 200 µm) as shown in Figure 2.5 was used to fabricate the membrane, after casting, the membrane left at the laboratory environment for 36 h to dry at room temperature, then it washed with distilled water 4 times to ensure completely removal of the solvent and kept for characterization process.

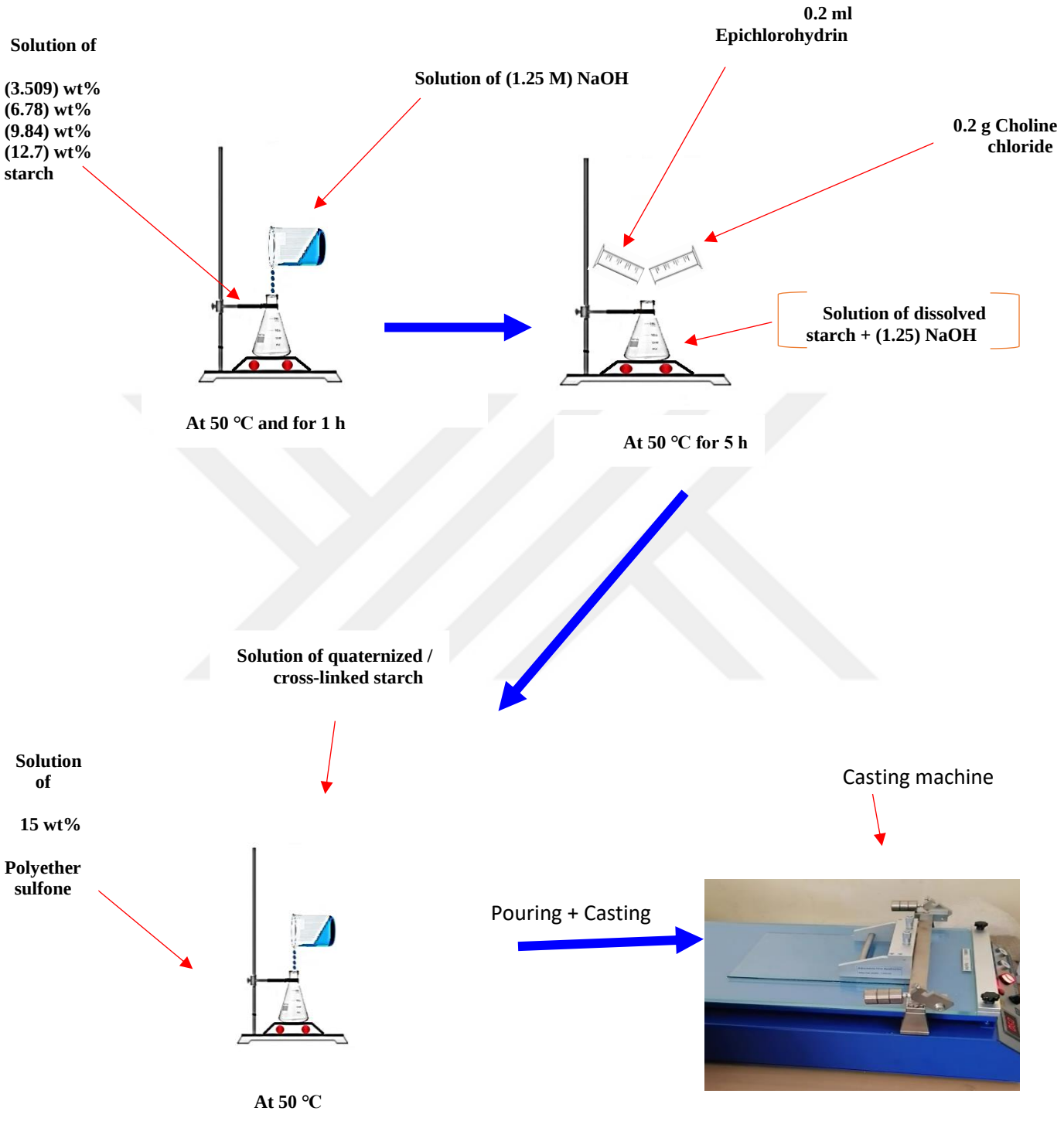

Figure 2.5 Schematic diagram of the dense membrane preparation.

2.4 Characterization

2.4.1 Scanning electron microscopy (SEM)

A scanning electron microscopy (SEM) measurement (TESCAN VEGA3 SB instrument, EO Elektronen-Optik-Service GmbH, Germany) was used to examine the top surface and cross-sectional morphology of the pristine membrane and the fabricated AEMs at an accelerating voltage of 10 Kv. The samples were prepared by drying for 12 h at 50 ℃ in oven before imaging. For cross-sectional images, the membrane was broken in liquid nitrogen to retain the membrane structure and then inspected using SEM equipment. The cross-section and outer surface of the membrane were scanned at several magnifications.

2.4.2 Fourier transform infrared (FTIR) analysis

Prior to perform FTIR analysis the fabricated AEMs were dried for 12 h at 50 ℃ in oven. Then, the fabricated AEMs are characterized by fourier transform infrared spectroscopy (FT-IR) in order to confirm the successful crosslinking, successful quaternization and successful blending with a tensor device (Bruker, Optik GmbH, Ettlingen, Germany) in the wavenumber range of 500-4000 cm^{-1} in transmittance mode.

2.4.3 Water uptake (WU), swelling ratio (SR)

Prior to perform this test The pristine polyether sulfone membrane and the fabricated AEM_s were dried for 12 h at 50 ℃ in oven and the mass and length were recorded. Followed by soaking in DI water for 24 h, after taking them out of the DI water they wiped with tissue paper and quikly the mass and length were measured. The WU can be calculated from the equation :

$$WU\ (\%) = [(W_{wet} - W_{dry})/(W_{dry})] \times 100\% \quad (4)$$

were W_{wet} and W_{dry} are the mass of the hydrated sample and dried sample, respectively. The SR can be determined from the following :

$$SR\ (\%) = [(l_{wet} - l_{dry})/(l_{dry})] \times 100\% \quad (5)$$

were l_{wet} and l_{dry} are the length of hydrated sample and dried sample, respective

CHAPTER 3

RESULTS AND DISCUSSION

3.1 Porous Polyether Sulfone Anion Exchange Membrane

3.1.1 Membrane morphology

The SEM images showing a surface and cross-section of the pristine polyether sulfone membrane and the fabricated AEMs are presented in Figures 3.1, 3.2, 3.3, 3.4, and 3.5 the pristine polyether sulfone and the fabricated AEMs were displayed the asymmetric structure consist of top layer and bottom as support layer. It is one of the membrane characteristics made via non-solvent induced phase separation technique. In Figure 3.1 the pristine polyether sulfone membrane showed an asymmetric morphology by the composition of a skin layer at the top and a support layer at the bottom. The thin top layer displays a spherulites-like structure with voids as shown in Figure 3.1b the thin top layer produced attribute to the good affinity of solvent DMSO to non-solvent (water).

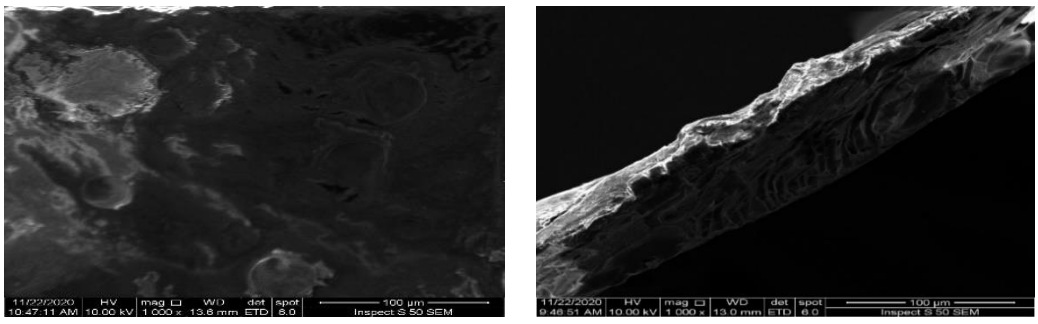

a) b)

Figure 3.1 SEM image of (a) Top surface (magnification ×1000) and (b) Cross-section (magnification ×1000) of pristine PES membrane.

When the membrane film was immersed into the coagulation bath, the DMSO has a good affinity towards the water. The high diffusion rate between DMSO and water leads the decreasing of polymer concentration in the surface and caused those voids. In Figure 3.1b the cross section displayed a little finger like structure as shown, there is large disruptive macro-voids in part of the cross-section. In Figure 3.2 Photo of pristine PES membrane as shown.

Figure 3.2 Photo of pristine PES membrane

Adding of quaternized/ crosslinked starch to the casting solution made a clear change in the membrane morphology, it led to smooth top surface as shown in Figure 3.3a also it resulted in thin finger like structure due to the lower diffusion rate between DMSO and water compare with pristine polyether sulfone membranebecause of the increasing in the casting solution viscosity as shown in Figure 3.3b.

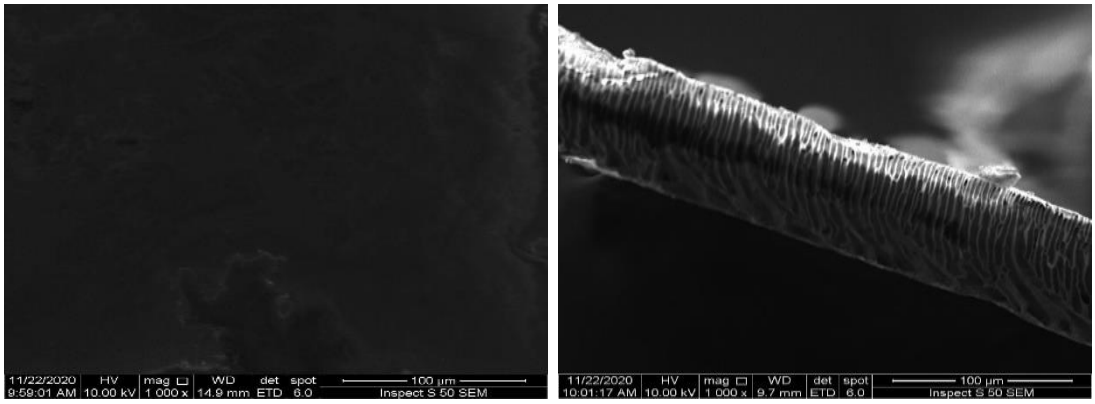

a) b)

Figure 3.3 SEM image of (a) Top surface (magnification ×1000) and (b) Cross-section image(magnification ×1000) of sample one (porous AEM with 3.509 wt% starch).

In Figure 3.4 Photo of sample 1 (porous AEM with 3.509 wt% starch) as shown.

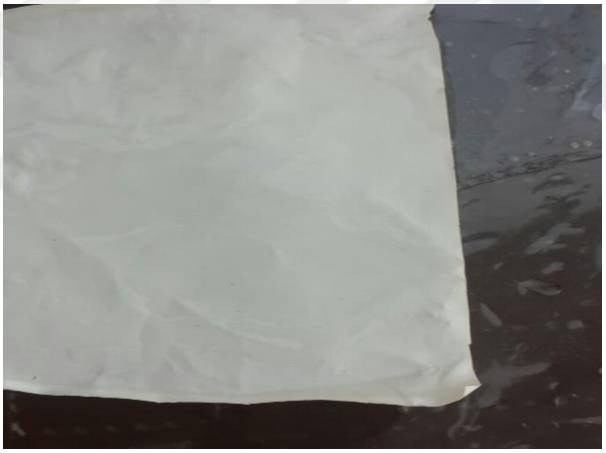

Figure 3.4 Photo of sample one (porous AEM with 3.509 wt% starch)

The required support layer should ideally serve as good mechanical support for the skin layer and should not give any additional transport resistance. Finger-like structure does not provide enough mechanical support for the skin layer, thin skin layer can rupture consequently facilitating AEM failure.

In Figure 3.5 asymmetric membrane as shown has been obtained. In Figure 3.5a further increasing in starch concentration caused a polymer separation as shown, there is a PES-rich phase and a quaternized/crosslinked ST-rich phase.

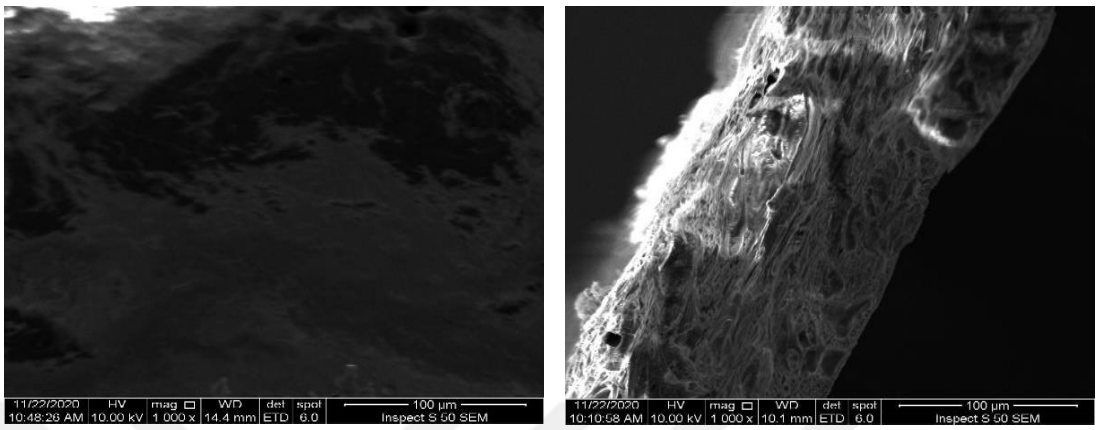

a) b)

Figure 3.5 SEM image of (a) Top surface (magnification ×1000) and (b) Cross section (magnification ×1000) of sample two (porous AEM with 6.78 wt% starch)

The whole cross-section displays spongy structure attribute to the increasing viscosity which caused slow precipitation as shown in Figure 3.5b.

In Figure 3.6 Photo of sample two (AEM with 6.78 wt% starch) as shown.

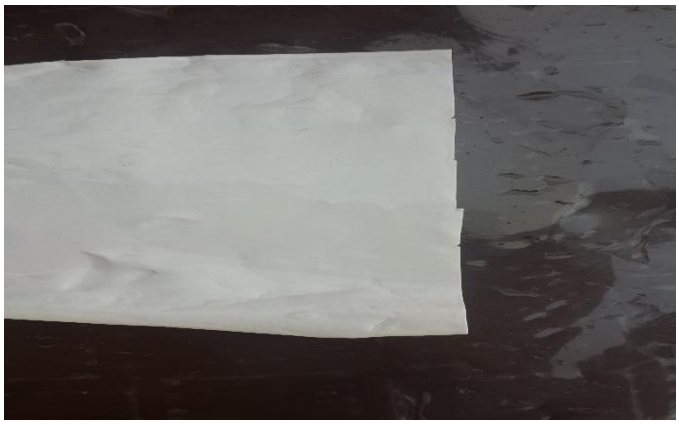

Figure 3.6 Photo of sample two (porous AEM with 6.78 wt% starch).

In Figure 3.7 asymmetric membrane has been obtained as shown.

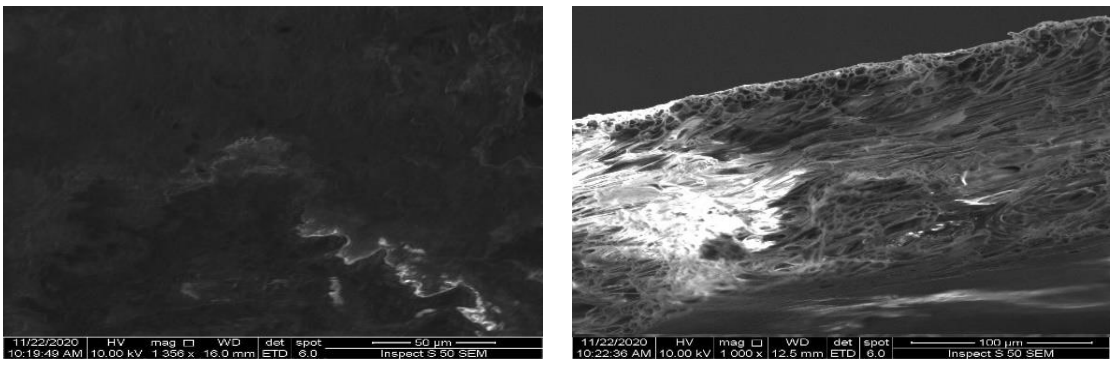

a) b)

Figure 3.7 SEM image of (a) Top surface (magnification ×1365) and (b) Cross section (magnification ×1000) of sample three (porous AEM with 9.84 wt% starch)

Increasing the starch concentration led to improve the ratio of starch/ epichlorohydrin in the casting solution, consequently, the fracture disappeared, the top surface becomes much smoother as shown in Figure 3.7a the support layer continues to display spongy-like structure as shown in Figure 3.7b.

In Figure 3.8 Photo of sample three (porous AEM with 9.84 wt% starch) as shown.

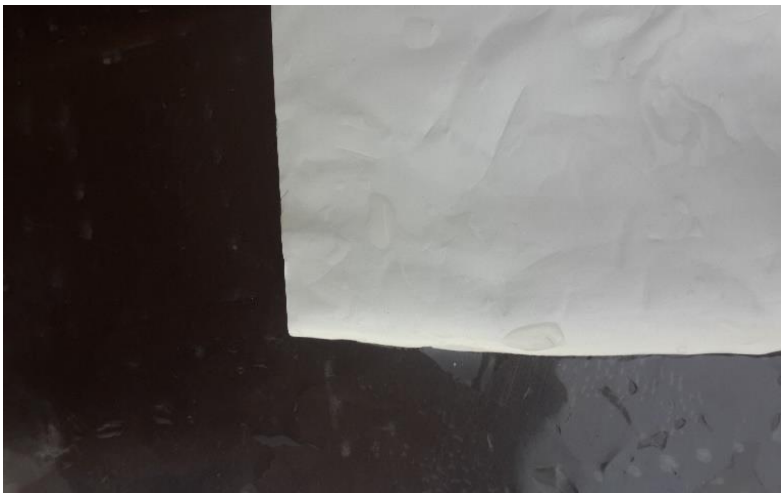

Figure 3.8 Photo of sample Three (porous AEM with 9.84 wt% starch).

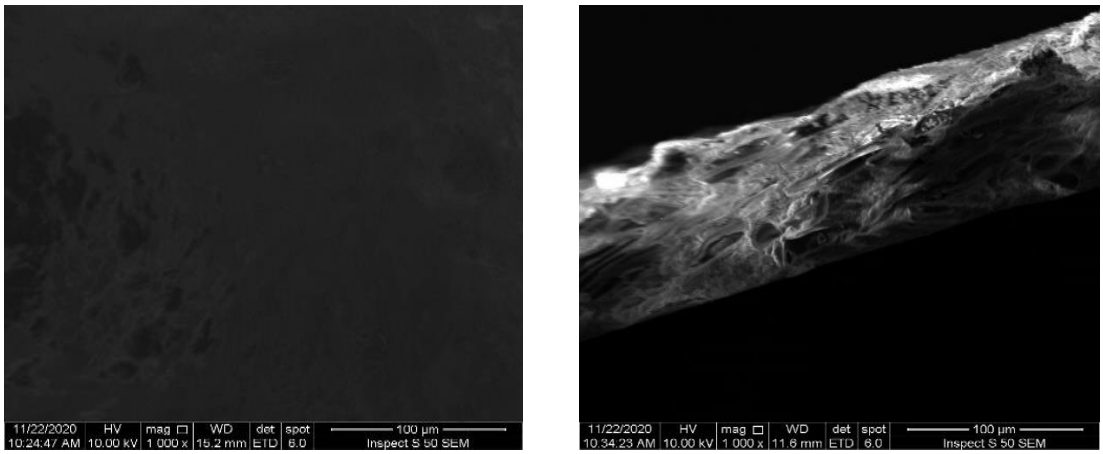

a) b)

Figure 3.9 SEM image of (a) Top surface (magnification ×1000) and (b) Cross section (magnification ×1000 of sample four (porous AEM with 12.7 wt% starch).

In Figure 3.9 asymmetric membrane as shown has been obtained. In Figure 3.9a smooth thin top layer as shown. In Figure 3.9b also the support layer displays the spongy-like structure as shown. Spongy-like structure is ideal because it gives good mechanical support to the skin layer.

In Figure 3.10 Photo of sample four (AEM with 12.7 wt% starch) as shown.

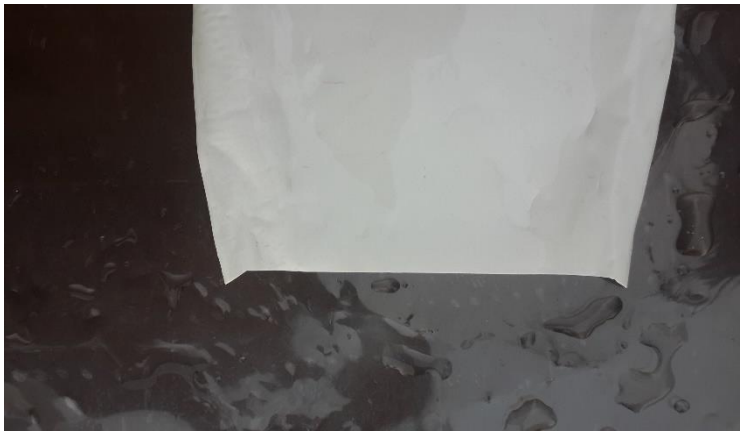

Figure 3.10 Photo of sample four (porous /AEM with 12.7 wt% starch).

3.1.2 FTIR analysis

We made FTIR spectrum for polyether sulfone powder and FTIR spectrums for the fabricated anion exchange membranes, then we looked at which new peaks are added to the polyether sulfone spectrum.

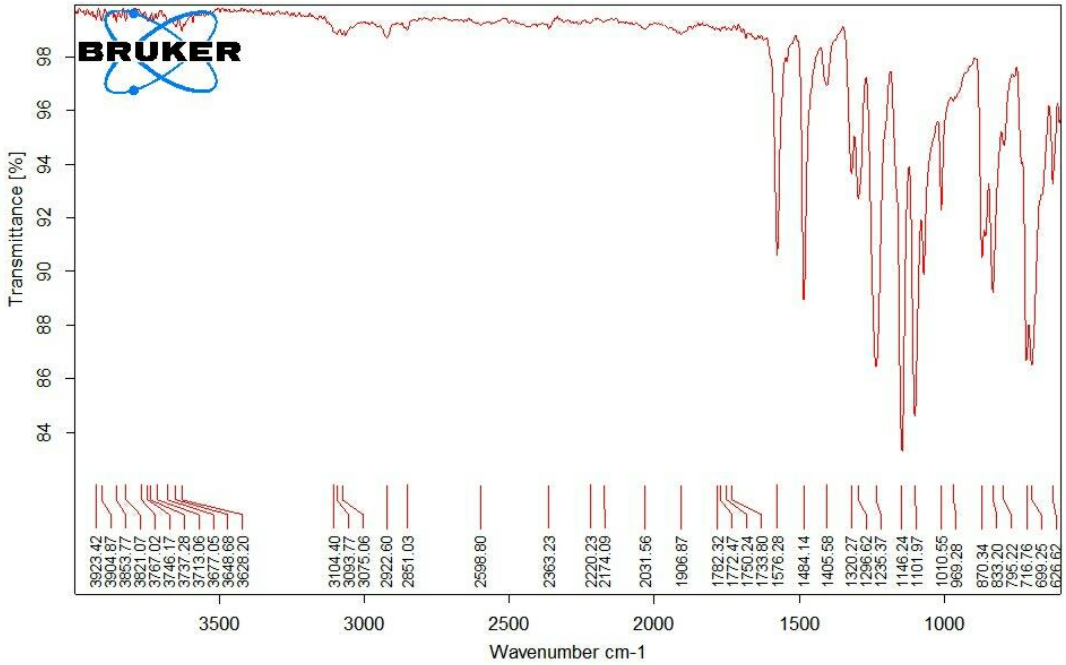

Figure 3.11 FTIR spectra of polyether sulfone powder.

The FTIR spectrum of the polyether sulfone powder which used to fabricate the AEMs as shown in Figure 3.11 displays S=O symmetric stretch at 1146.24 cm^{-1}, C-SO_2-C asymmetric stretch at 1320.27 cm^{-1}, C-O asymmetric at 1235.37 cm^{-1}, C_6H_6 ring stretch at 1484.14-1576.28 cm^{-1}, C-S group at 716.76 cm^{-1}.

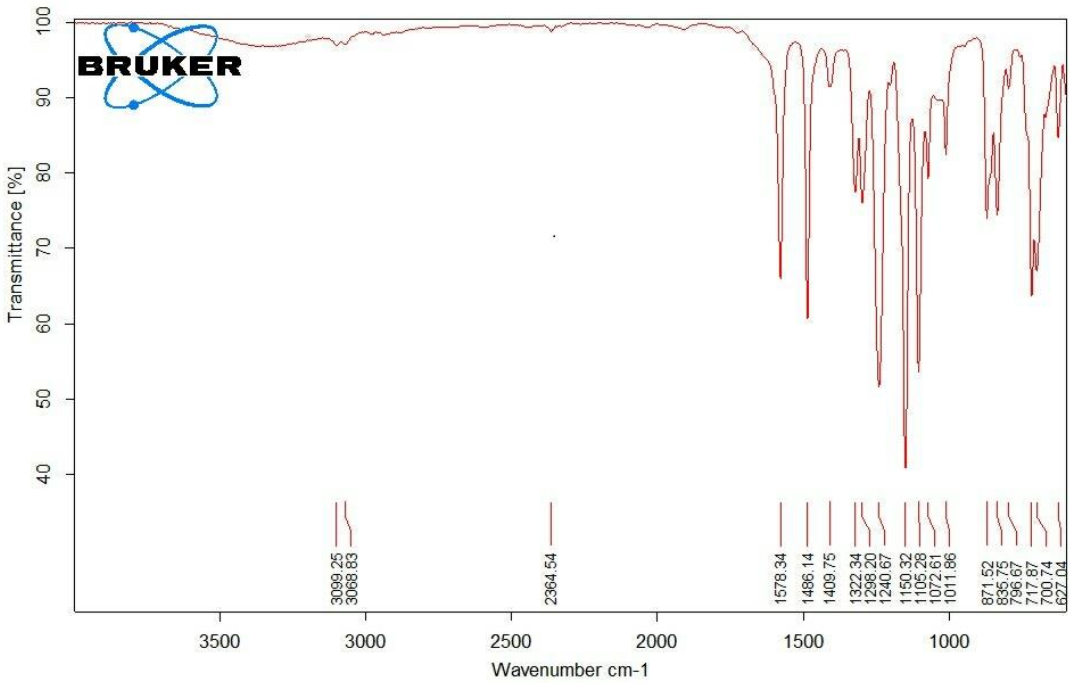

Figure 3.12 FTIR spectra of sample one (porous AEM with 3.509 wt% starch)

The FTIR spectrum of sample one (porous AEM with 3.509 wt% starch) as shown in Figure 3.12 displays a new peak at 3390-3400 cm^{-1} which are corresponds to the stretching vibration of O-H group. The new band at 1072.61 cm^{-1} is assignable to the C-O-C stretching vibration, which is clear proof of the successful crosslinking. The new peak near 960 cm^{-1} is assignable to the C-N stretching vibration. The stretching vibration of the CH_3 groups in trimethylammonium $(CH_3)_3N$ are at 3099.25-3068.83 cm^{-1}, that which is clear proof of the successful incorporation of the quaternary ammonium head groups. The bands at around 2900 cm^{-1} and at around 2800 cm^{-1} seem to be related to the CH_2 and CH groups of the hydroxypropyl bridges. The spectrum also displays polyether sulfone functional groups: S=O symmetric stretch at 1150.32 cm^{-1}, C-SO_2-C asymmetric stretch at 1322.34 cm^{-1}, C-O asymmetric at 1240.67 cm^{-1}, C_6H_6 ring stretch at 1486.14-1587.34 cm^{-1}, C-S group at 717.87 cm^{-1}.

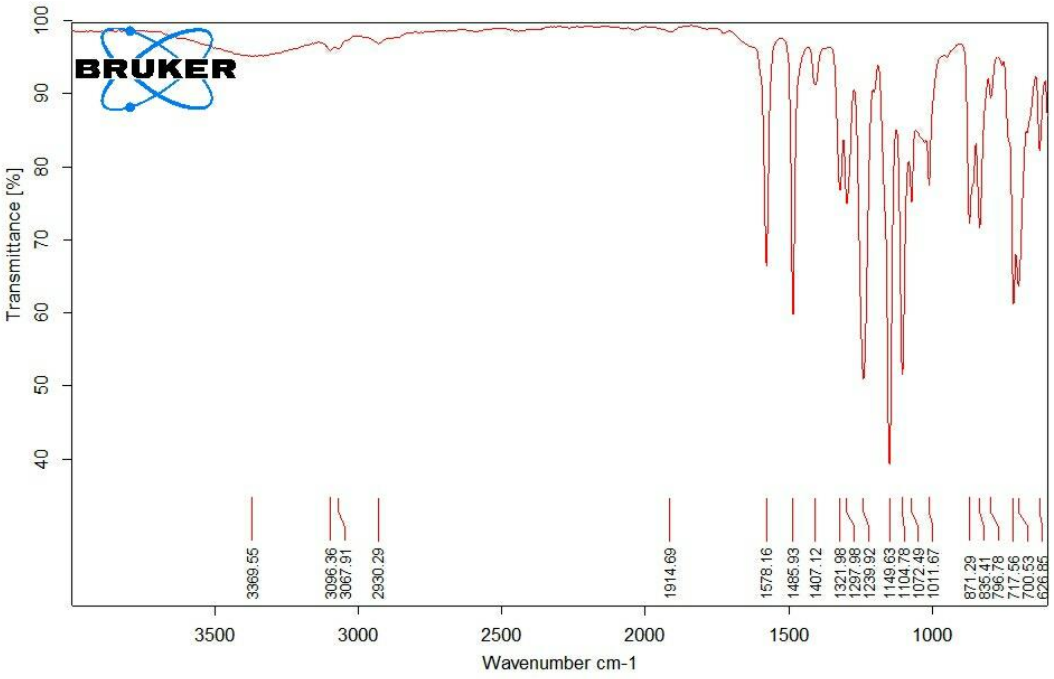

Figure 3.13 FTIR spectra of sample two (porous AEM with 6.78 wt% starch)

The FTIR spectrum of sample two (porous AEM with 6.78 wt% starch) as shown in Figure 3.13 displays a peak between 3369.55 cm^{-1} which are corresponds to the stretching vibration of O-H group. The band at 1072.49 cm^{-1} is assignable to the C-O-C stretching vibration, which is clear proof of the successful crosslinking. The peak between 940-950 cm^{-1} is assignable to the C-N stretching vibration. The stretching vibration of the CH_3 groups in trimethylammonium $(CH_3)_3N$ are at 3096.36-3067.91 cm^{-1}, that which is clear proof of the successful incorporation of the quaternary ammonium head groups. The bands at 2930.29 cm^{-1} and near 2800 cm^{-1} seem to be related to the CH_2 and CH groups of the hydroxypropyl bridges. The spectrum also displays polyether sulfone functional groups: S=O symmetric stretch at 1149.63 cm^{-1}, C-SO_2-C asymmetric stretch at 1321.98 cm^{-1}, C-O asymmetric at 1239.92 cm^{-1}, C_6H_6 ring stretch at 1485.93-1578.16 cm^{-1}, C-S group at 717.56 cm^{-1}.

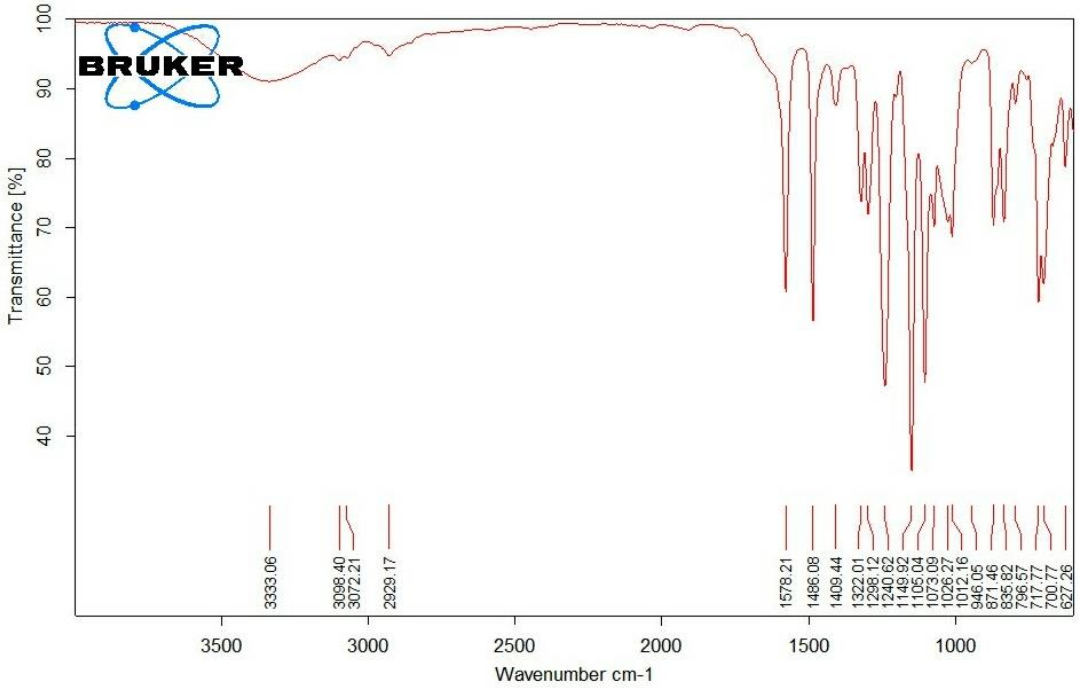

Figure 3.14 FTIR spectra of sample three (porous AEM with 9.84 wt% starch).

The FTIR spectrum of sample three (porous AEM with 9.84 wt% starch) as shown in Figure 3.14 displays a peak at 3333.06 cm^{-1} which are corresponds to the stretching vibration of O-H group. The band at 1073.09 cm^{-1} is assignable to the C-O-C stretching vibration, which is clear proof of the successful crosslinking. The peak at 946.05 cm^{-1} is assignable to the C-N stretching vibration. The stretching vibration of the CH_3 groups in trimethylammonium $(CH_3)_3N$ are at 3098.40-3072.21 cm^{-1}, that which is clear proof of the successful incorporation of the quaternary ammonium head groups. The bands at 2929.17cm^{-1} and at around 2800 cm^{-1} seem to be related to the CH_2 and CH groups of the hydroxypropyl bridges. The spectrum also displays polyether sulfone functional groups: S=O symmetric stretch at 1149.92 cm^{-1}, C-SO_2-C asymmetric

stretch at 1322.01 cm^{-1}, C-O asymmetric at 1240.62 cm^{-1}, C_6H_6 ring stretch at 1486.08-1578.21 cm^{-1}, C-S group at 717.77 cm^{-1}.

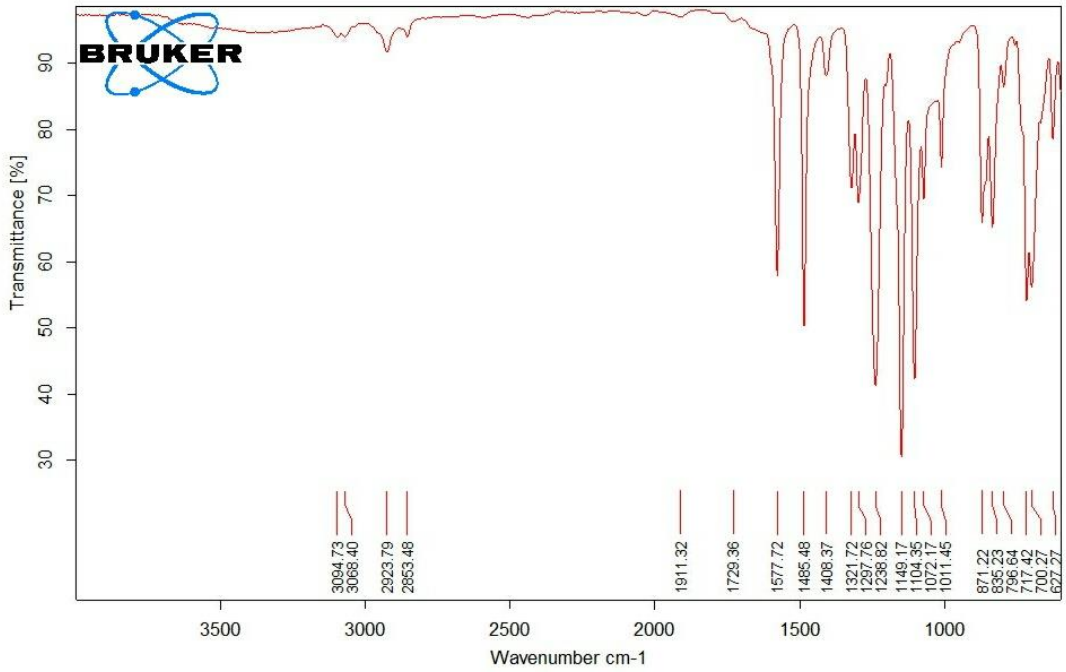

Figure 3.15 FTIR spectra of sample four (porous AEM with 12.7 wt% starch).

The FTIR spectrum of sample four (AEM with 12.7 wt% starch) as shown in Figure 3.15 displays a peak between 3900-4000 cm^{-1} which are corresponds to the stretching vibration of O-H group. The band at 1072.47 cm^{-1} is assignable to the C-O-C stretching vibration, which is clear proof of the successful crosslinking. The peak between 940-950 cm^{-1} is assignable to the C-N stretching vibration. The stretching vibration of the CH_3 groups in trimethylammonium $(CH_3)_3N$ are at 3094.73-3068.40 cm^{-1}, that which is clear proof of the successful incorporation of the quaternary ammonium head groups. The bands at 2923.79 cm^{-1} and at 2853.48 cm^{-1} seem to be related to the CH_2 and CH groups of the hydroxypropyl bridges. The spectrum displays polyether sulfone functional groups: S=O symmetric stretch at 1149.17 cm^{-1}, C-SO_2-C asymmetric stretch at 1321.72 cm^{-1}, C-O asymmetric at 1238.82 cm^{-1}, C_6H_6 ring stretch at 1485.48-1577.72 cm^{-1}, C-S group at 717.42 cm^{-1}. The four spectrums are similar, only there is a small shifts in the wave number positions which these (small shifts) in turn, confirm that there is only physical blending happened between the quaternized/ crosslinked starch and the polyether sulfone, in other words it means the successful blending between the quaternized/ crosslinked starch and the polyether sulfone.

3.1.3 Water uptake (WU) and swelling ratio (SR)

Hydroxide ion conductivity of any AEM has strong reliance on the associated water uptake, sufficient water uptake is necessary to reach high ionic conductivity. On the other hand, the excessive water uptake will lead to the membrane swelling problem. The results of Table 3.1 reveal high water uptake levels were obtained which will lead to high ion exchange capacity and eventually will result in reaching high ionic conductivity. The results also confirmed that we succeeded to overcome the swelling problem which normally be associated with the high levels of water uptake. The dimensional stability of polyether sulfone and the efficient crosslinking for starch were the two reasons behind keeping the water swelling ratio at very low values (0.76% for sample one, 5.3% for sample two, 2.56% for sample three, 3.9% for sample four), these results reveal that the fabricated AEMs in this work are mechanically robust. Regarding the thickness of the fabricated AEMs we saw that the thickness was 83.33 µm for sample one (AEM with 3.509 wt % starch) and then increased, this increasing in thickness was mainly to the increasing in hydrogen bonding between the oxygen atom of sulfonic group and the hydroxyl group of starch, the hydrogen bonding caused the increasing in the dope solution viscosity which in turn resulted in the membrane thickness increasing. But for sample four (AEM with 12.7 wt % starch) we saw the thickness is decreased greatly (from 166.67 µm to 104.16 µm) due the great reduction in hydrogen bonding, all hydroxyl groups were etherified and converted into hydroxypropyl groups which led to decrease the dope solution viscosity eventually decreasing in the membrane thickness.

Table 3.1 Water uptake (WU) and swelling ratio (SR) of the porous AEMs.

Sample Name	Water Uptake (WU%)	Swelling Ratio (SR%)	Thickness (μm)
Sample one (porous AEM with 3.509 wt% starch)	107.46	0.76	83.33
Sample two (porous AEM with 6.78 wt% starch)	376.7	5.3	133.33
Sample three (porous AEM with 9.84 wt% starch)	329	2.56	166.67
Sample four (porous AEM with 12.7 wt % starch)	345.7	3.9	104.17

In Table 3.2 as shown we made comparison between our fabricated porous AEM and the CEM fabricated by Hamid et al. [80] in terms of thickness and water uptake.

Table 3.2. Comparison between the fabricated porous AEM and the porous CEM of [80].

	Thickness (µm)	Water Uptake (WU%)
Porous anion exchange membrane (This work)	133.33	376.7
Porous cation exchange membrane Hamid et al. [80]	170	550

3.2 Dense Polyether Sulfone Anion Exchange Membrane

3.2.1 Membrane morphology

The SEM images showing a surface and cross-section of the fabricated AEMs are presented in Figures 3.16, 3.18, 3.20 and 3.22.

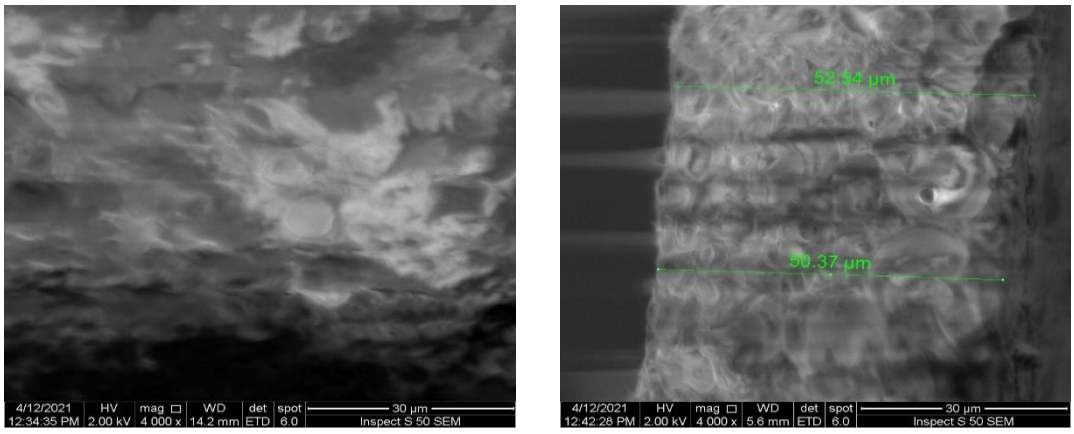

a) b)

Figure 3.16 SEM image of (a) Top surface (magnification ×4000) and (b) Cross-section (magnification ×4000) of sample one (dense AEM with 3.509 wt% starch).

In Figure 3.16 b there is a dense top layer, also the cross section image exhibited dense structure as shown.\

In Figure 3.17 Photo of sample one (dense AEM with 3.509 wt% starch) as shown.

Figure 3.17 Photo of sample one (dense AEM with 3.509 wt% starch).

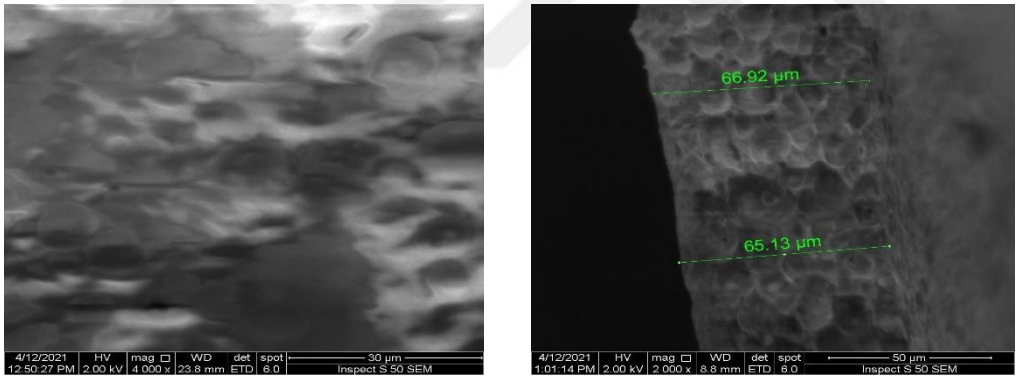

a) b)

Figure 3.18 SEM image of (a) Top surface (magnificati on ×4000) and (b) Cross-section (magnification ×2000) of sample two (dense AEM with 6.78 wt% starch).

Add more starch led to increase the viscosity of the dope solution which in turn resulted in the increasing of the membrane thickness. No much changes in the morphology after adding more quaternized/crosslinked starch as shown in Figure 3.18 a and 3.18 b the dense structue is clear.

In Figure 3.19 Photo of sample two (dense AEM with 6.78 wt% starch) as shown.

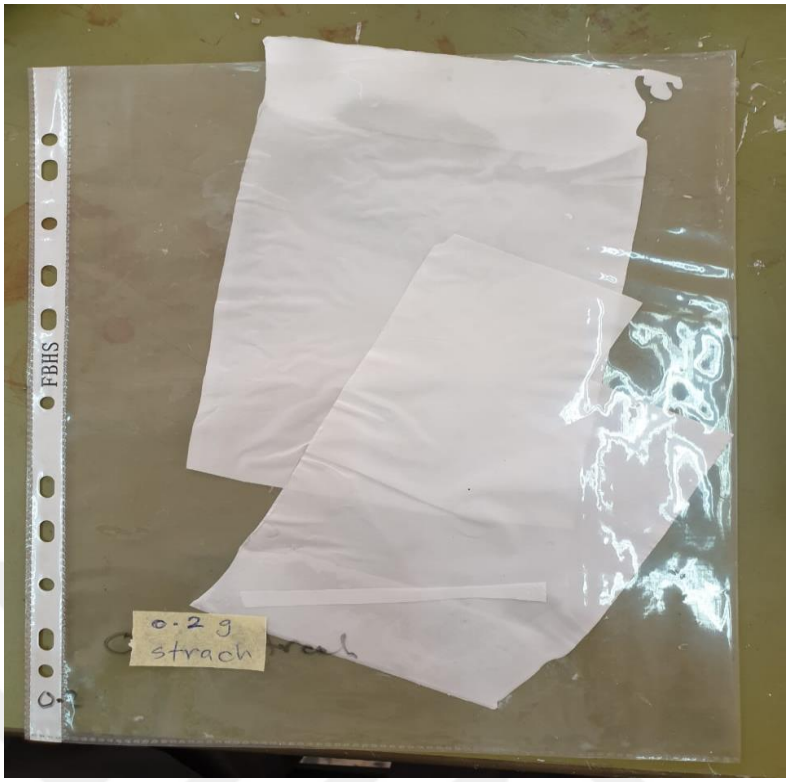

Figure 3.19 Photo of sample two (dense AEM with 6.78 wt% starch).

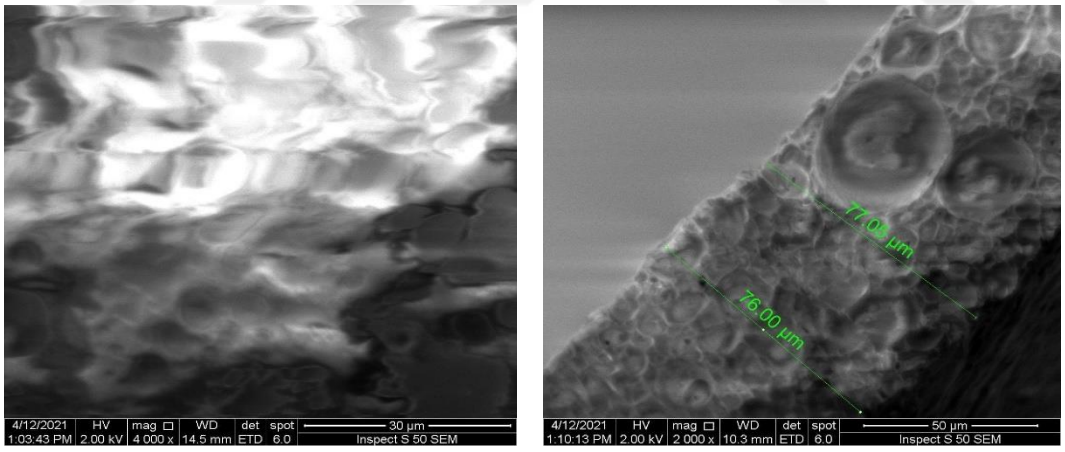

a) b)

Figure 3.20 SEM image of (a) Top surface (magnification ×4000) and (b) Cross-section (magnification ×2000) of sample three (dense AEM with 9.84 wt% starch).

again add more starch led to increase the membrane thickness As shown in Figure 3.20 a we can see more rough top layer, as shown in figure 3.20 b the cross-scection displays dense structure.

In Figure 3.21 Photo of sample three (dense AEM with 9.84 wt% starch) as shown.

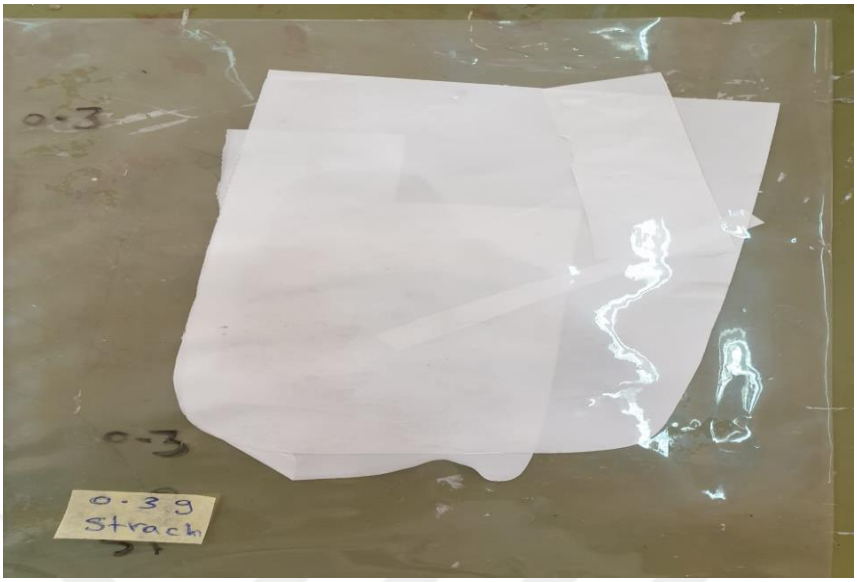

Figure 3.21 Photo of sample three (dense AEM with 9.84 wt% starch).

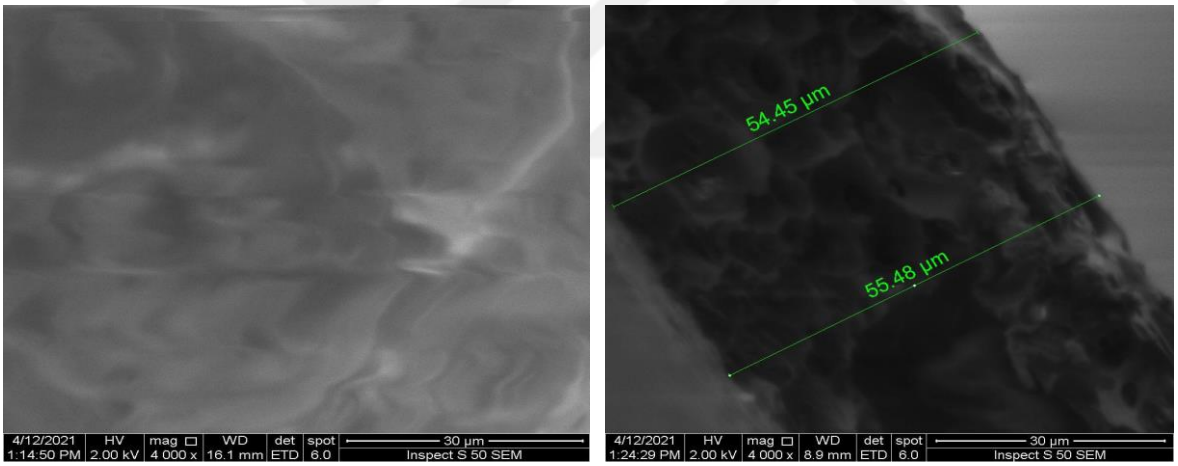

a) b)

Figure 3.22 SEM image of (a) Top surface (magnification ×4000) and (b) Cross-section (magnification ×4000) of sample four (dense AEM with 12.7 wt% starch).

In Figure 3.22 a and 3.22 b as shown anion membrane with dense and smooth surface, also this indicates the high compatibility between polyether sulfone and starch.

In Figure 3.23 real photo of sample four (dense AEM with 12.7 wt% starch) as shown.

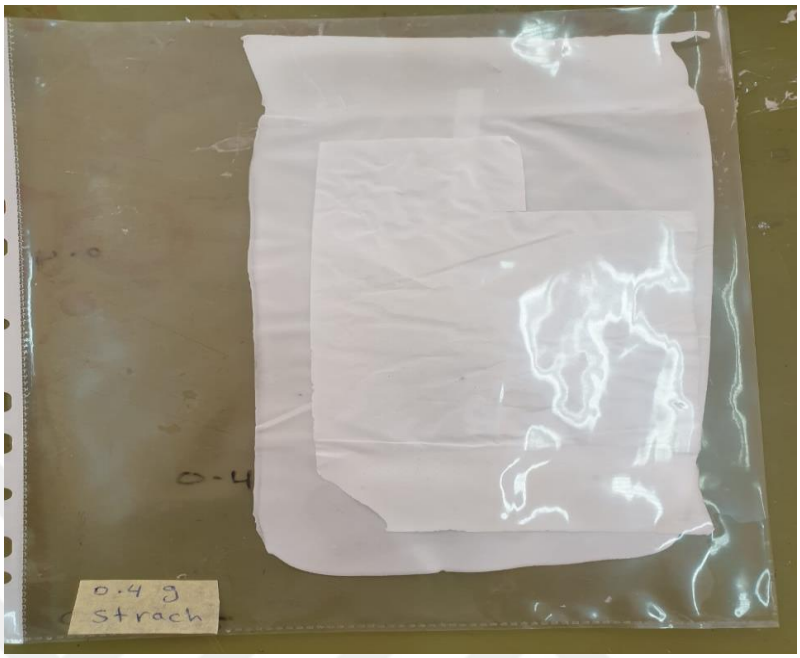

Figure 3.23 Photo of sample four (dense AEM with 12.7 wt% starch).

3.2.2 FTIR analysis

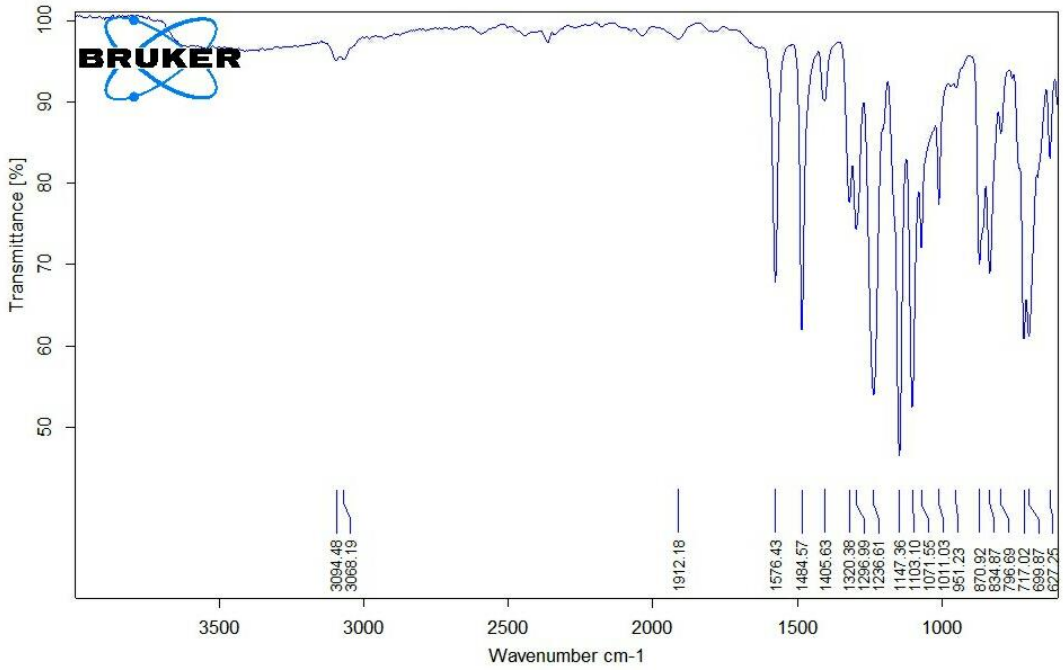

Figure 3.24 FTIR spectra of sample one (dense AEM with 3.509 wt% starch).

The FTIR spectrum of sample one (dense AEM with 3.509 wt% starch) as shown in Figure 3.24 displays a new peak between 3390-3400 cm^{-1} which are corresponds to the stretching vibration of O-H group. The new band at 1071.55 cm^{-1} is assignable to the C-O-C stretching vibration, which is clear proof of the successful crosslinking. The new peak at 951.23 cm^{-1} is assignable to the C-N stretching vibration. The stretching vibration of the CH_3 groups in trimethylammonium $(CH_3)_3N$ are at 3094.48-3068.19 cm^{-1}, that which is clear proof of the successful incorporation of the quaternary ammonium head groups. The bands at around 2900 cm^{-1} and at around 2800 cm^{-1} seem to be related to the CH_2 and CH groups of the hydroxypropyl bridges. The spectrum also displayed functional groups specific to polyether sulfone: S=O symmetric stretch at 1147.36 cm^{-1}, C-SO_2-C asymmetric stretch at 1320.38 cm^{-1}, C-O asymmetric at 1236.61 cm^{-1}, C_6H_6 ring stretch at 1484.57-1578.43 cm^{-1}, C-S group at 717.02 cm^{-1}.

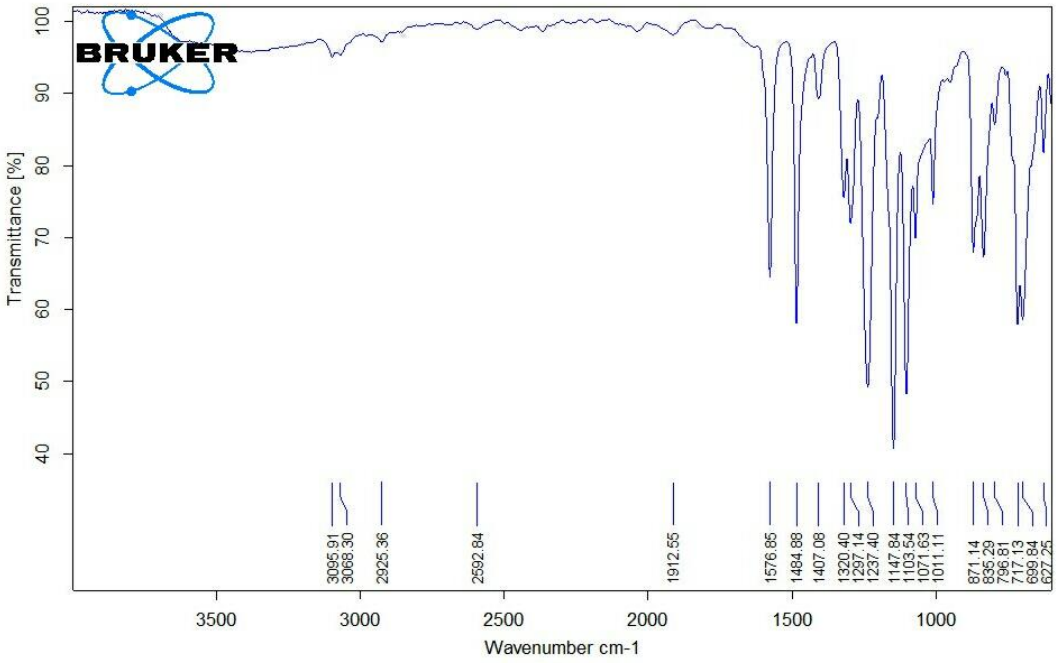

Figure 3.25 FTIR spectra of sample two (dense AEM with 6.78 wt% starch).

The FTIR spectrum of sample two (dense AEM with 6.78 wt% starch) as shown in Figure 3.25 displays a peak between 3390-3400 cm^{-1} which are corresponds to the stretching vibration of O-H group. The band at 1071.63 cm^{-1} is assignable to the C-O-C stretching vibration, which is clear proof of the successful crosslinking. The peak near 950 cm^{-1} is assignable to the C-N stretching vibration. The stretching vibration of

the CH_3 groups in trimethylammonium $(CH_3)_3N$ are at 3095.91-3068.30 cm^{-1}, that which is clear proof of the successful incorporation of the quaternary ammonium head groups. The bands at 2925.36 cm^{-1} and at around 2800 cm^{-1} seem to be related to the CH_2 and CH groups of the hydroxypropyl bridges. The spectrum also displayed functional groups specific to polyether sulfone: S=O symmetric stretch at 1147.84 cm^{-1}, C-SO_2-C asymmetric stretch at 1320.40 cm^{-1}, C-O asymmetric at 1237.40 cm^{-1}, C_6H_6 ring stretch at 1484.88-1576.85 cm^{-1}, C-S group at 717.13 cm^{-1}.

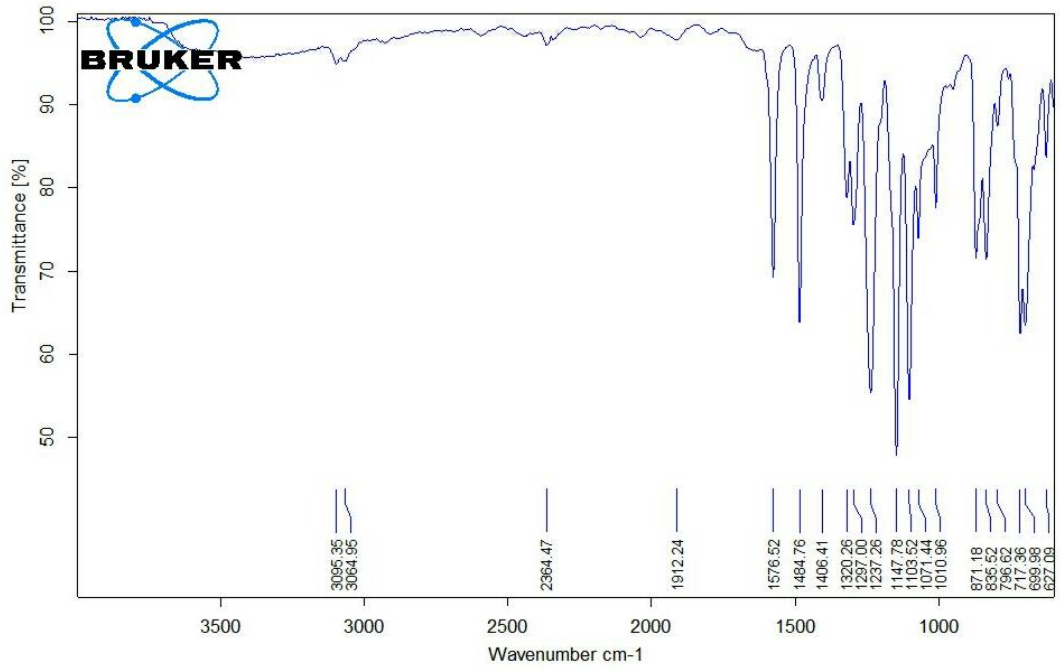

Figure 3.26 FTIR spectra of sample three (dense AEM with 9.78 wt% starch).

The FTIR spectrum of sample three (dense AEM with 9.84 wt% starch) as shown in Figure 3.26 displays a peak between 3390-3400 cm^{-1} which are corresponds to the stretching vibration of O-H group. The band at 1071.44 cm^{-1} is assignable to the C-O-C stretching vibration, which is clear proof of the successful crosslinking. The peak near 950 cm^{-1} is assignable to the C-N stretching vibration. The stretching vibration of the CH_3 groups in trimethylammonium $(CH_3)_3N$ are at 3095.35-3064.95 cm^{-1}, that which is clear proof of the successful incorporation of the quaternary ammonium head groups. The bands at around 2900 cm^{-1} and at around 2800 cm^{-1} seem to be related to the CH_2 and CH groups of the hydroxypropyl bridges. The spectrum also displayed functional groups specific to polyether sulfone : S=O symmetric stretch at 1147.78 cm^{-}

[1], C-SO_2-C asymmetric stretch at 1320.26 cm^{-1}, C-O asymmetric at 1237.26 cm^{-1}, C_6H_6 ring stretch at 1484.76-1576.52 cm^{-1}, C-S group at 717.36 cm^{-1}.

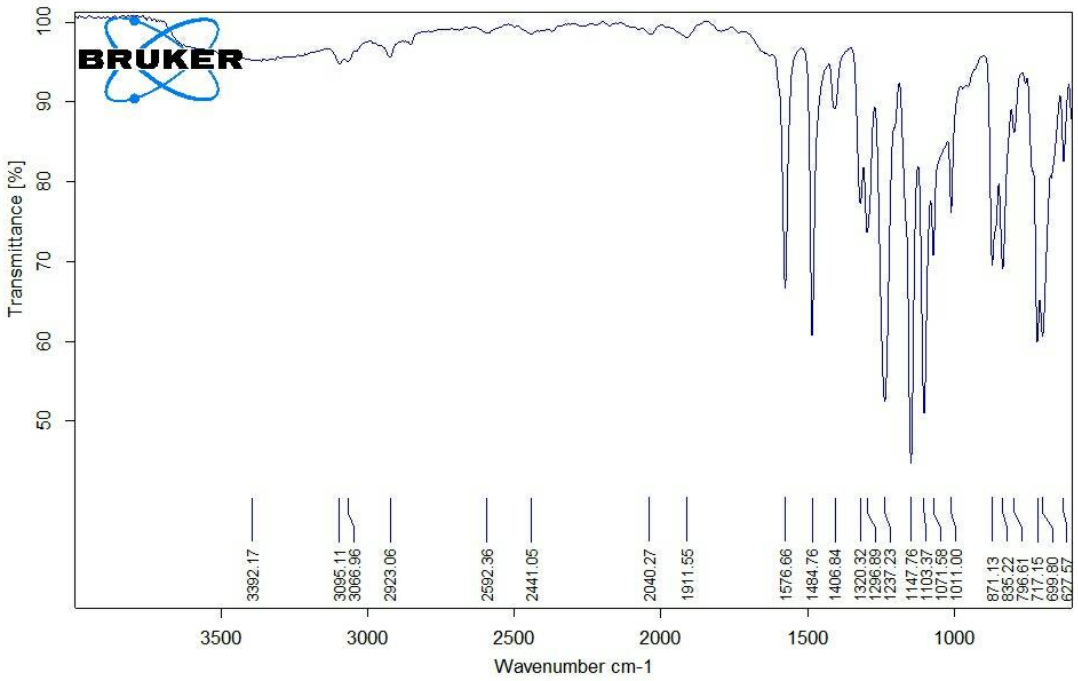

Figure 3.27 FTIR spectra of sample four (dense AEM with 12.7 wt% starch).

The FTIR spectrum of sample four (dense AEM with 12.7 wt% starch) as shown in Figure 3.27 displays a peak at 3392.17 cm^{-1} which are corresponds to the stretching vibration of O-H group. The band at 1071.58 cm^{-1} is assignable to the C-O-C stretching vibration, which is clear proof of the successful crosslinking. The peak near 950 cm^{-1} is assignable to the C-N stretching vibration. The stretching vibration of the CH_3 groups in trimethylammonium $(CH_3)_3N$ are at 3095.11-3066.96 cm^{-1}, that which is clear proof of the successful incorporation of the quaternary ammonium head groups. The bands at 29232.06 cm^{-1} and near 2800 cm^{-1} seem to be related to the CH_2 and CH groups of the hydroxypropyl bridges. The spectrum also displayed functional groups specific to polyether sulfone: S=O symmetric stretch at 1147.76 cm^{-1}, C-SO_2-C asymmetric stretch at 1320.32 cm^{-1}, C-O asymmetric at 1237.23 cm^{-1}, C_6H_6 ring stretch at 1484.76-1576.66 cm^{-1}, C-S group at 717.15 cm^{-1}. The four spectrums are similar, only there is a small-shifts, which these small shifts in turn confirm that there is only physical blending happened between the quaternized/ crosslinked starch and the

polyether sulfone, in other words it means the successful blending between the quaternized/ crosslinked starch and the polyether sulfone.

3.2.3 Water uptake (WU) and swelling (SR) ratio

The results of Table 3.2 reveal very good water uptake levels were obtained which in turn will lead to high ion exchange capacity and eventually will result in reaching high ionic conductivity. The results confirm that our fabrication route to fabricate the AEMs was very successful.

Table 3.3 Water uptake (WU) and swelling ratio of the dense AEMs.

Sample Name	Water Uptake (WU%)	Swelling Ratio (SR%)	Thickness (µm)
Sample one (AEM with 3.509 wt% starch)	49.7	2.7	52.54
Sample two (AEM with 6.78 wt% starch)	61	3.33	66.92
Sample three (AEM with 9.84 wt% starch)	68.4	5	77.05
Sample four (AEM with 12.7 wt % starch)	69.9	7.5	55.48

In Table 3.3 as shown we made a comparison between the semi-IPN developed in this thesis and IPN of Lingping et al. [46].

Table 3.4 Comparison between the developed semi-IPN in this thesis and IPN of [46].

	Thickness (µm)	Water Uptake (WU%)	Swelling Ratio (SR%)
Semi-IPN of polyether sulfone/ quaternized starch (This work)	55.48	69.9	7.5
Fully IPN of crosslinked PVA/ crosslinked poly (vinyl benzyl-N-methyl piperidinium) Lingping et al. [46]	40	67.5	11

CHAPTER 4

CONCLUSION

Adding porosity to the AEM contributed massively to the increasing of water uptake. Water uptake of the dense polyether sulfone AEM was 69.9% while for the porous polyether sulfone AEM was 376.7%. This was attributed to the increasing of the free volume. Excellent result represented by keeping the swelling ratio at low values as 5.3% for the porous polyether sulfone AEM and 7.5% for the dense polyether sulfone AEM, which was attributed to the combination of poly ether sulfone's exceptional dimensional stability and the efficient crosslinking with starch. Semi-interpenetrating polymer network (semi-IPN) is one of the best fabrication routes to avoid the problems associated with the fabrication of homogeneous AEMs (e.g. carcinogenic-chemicals problem and high-cost fabrication problem), and also to avoid the problems associated with the fabrication of heterogeneous AEMs (e.g. thickness problem and non-uniform structure problem). The sufficient water uptake levels of the AEMs fabricated in this work undoubtedly will lead to high amount of an ion exchange capacity which in turn will result in high ionic conductivity. The combination of expected high ionic conductivity and the very low swelling ratio achieved makes the fabricated AEMs in this work attractive for alkaline fuel cell applications. Polyether sulfone with its excellent dimensional stability and excellent chemical stability can be exploited to fabricate AEMs with high stability. Polysaccharide family polymers with its excellent hydrophilic properties and with its easy modification process can be exploited to a great extent to fabricate AEMs with high ionic conductivity. Epichlorohydrin is amazing crosslinking agent for the polysaccharide family polymers, it enables these polymers to overcome its poor mechanical properties and becomes suitable for many applications.

REFERENCES

[1] H. Huang, Z. Du, Y. He, "The effect of population expansion on energy consumption in canton of china: A simulation from computable general equilibrium approach." *International Journal of Engineering Sciences & Management Research,* vol. 5, pp. 19-26, 2018.

[2] I. Dincer, "Energy and environmental impacts: Present and future perspectives." *Energy Sources Journal*, Vol. 20, pp. 427-453, 1998.

[3] J. Thomas, P. Edwards, P. Dobson, G. Owen, "Decarbonising energy: The developing international activity in hydrogen technologies and fuel cells." *Journal of Energy Chemistry*, vol. 51, pp. 405-415, 2020.

[4] D. Ibrahim, "Hydrogen and fuel cell technologies for sustainable future." *JJMIE*, vol. 2, pp. 1-14, 2008.

[5] G. Leonardo, L. Fabio, "Fuel cells: technologies and applications." *The Open Fuel Cells Journal*, vol. 1, pp. 1-20, 2013.

[6] Z. Xing, "Current status of stationary fuel cells for coal power generation." *Clean Energy Journal*, vol. 2, pp. 126-139, 2018.

[7] N. Meng, "Current status of fuel cell technologies." *Energy Exploration and Exploitation*, vol. 23, pp. 207-214, 2005.

[8] Y. Wang, K. Chen, J. Mishler, S. Cho, X. Adroher, “A review of polymer electrolyte membrane fuel cells: Technology, applications, and needs on fundamental research” *Applied Energy Journal,* vol. 88, pp. 981-1007, 2011.

[9] L. Shanfu, P. Jing, H. Aibin, Z. Lin, L. Juntao, “Alkaline polymer electrolyte fuel cells completely free from noble metal catalysts.” *PMC Journal*, vol. 105, pp. 20611-20614, 2008.

[10] H. Garrete, M. Mrinmay, P. Xiong, C. Ami, S. Bryan, E. William. Mustain, A. Paul, “Composite poly(norbornene) anion conducting membrane for acheiving durability water management and high power (3.4 W/cm^2) in hydrogen/oxygen alkaline fuel cells.” *ECS Journal*, vol. 166, pp. 637-644, 2019.

[11] W. Billy, M. Mardit, J. Gregory, “Hydrogen PEMFC system for automotive applications.” *International Journal of Low-Carbon Technologies,* vol. 7, pp. 28-37, 2012.

[12] Z. Xiangyang, J. Hao, L Bing, C. Zhang, “High-repetitive reversal tolerant performance of proton-exchange membrane fuel cell by designing a suitable anode.” *ACS Omega,* vol. 5, pp. 10099-10105, 2020.

[13] M. Junpei, W. Masahiro, M. Kenji, “Ammonium-functionalized poly (arylene ether) as anion-exchange membranes.” *Polymer Journal*, vol. 46, pp. 656-663, 2014.

[14] N. Syarifah, J. Juhana, N. Muhammad, S. Rubita, “Poly (ether ether ketone) based anion exchange membrane for solid alkaline fuel cell: a review.” *Journal of Membrane Science and Research,* vol. 5, pp. 205-215, 2019.

[15] A. Horie, E. William, “Catalytic advantages, challenges, and priorities in alkaline membrane fuel cells.” *American Chemical Society Journal,* vol. 10 pp. 225-234, 2019.

[16] M. Sandip, H. Sung, K. Yekyung, H. Seung, “A review on recent developments of anion exchange membranes for fuel cells and redox flow batteries.” *RSC Advances Journal,* vol. 5, pp. 37206-37230, 2015.

[17] Y. Wei, P. Elliot, N. Samantha, A. David, W. Geoffrey, “Highly conductive and chemically stable alkaline anion exchange membranes via ROMP of trans-cyclooctane derivatives.” *PNAS Journal,* vol. 116, pp. 9729-9734, 2019.

[18] X. Tongwen, W. Yng, “Fundamental studies of a new series of anion exchange membranes: membrane preparation and characterization.” *Journal of Membrane Science*, vol. 190, pp. 159-166, 2001.

[19] G. Mclean, T. Niet, S. Prince-Richard, N. Djilali, “An assessment of alkaline fuel cell technology.” *International Journal of Hydrogen Energy*, vol. 27, pp. 507-526, 2002.

[20] B. Smitha, S. Srihar, A. Khan, “Solid polymer electrolyte membranes for fuel cell applications-a review.” *Journal of Membrane Science,* vol. 259, pp. 10-26, 2005.

[21] J. Yan, M. Hickner, “Anion exchange membranes by bromination of benzylmethyl-containing poly(sulfone)s.” *Macromolecules Journal,* vol. 43 pp. 2349-2356, 2010.

[22] C. Zhao, Y. Gong, Q. Liu, Q. Zhang, A. Zhu, “Self-crosslinked /anion exchange membranes by bromination of benzylmethyl-containing

poly(sulfone)$_s$ for direct methanol fuel cells." *International Journal of Hydrogen Energy*, vol. 37 pp. 11383-11393, 2012.

[23] I. Wenten, Khoiruddin, "Recent development in heterogeneous ion-exchange membrane: preparation , modification, characterization and performance evaluation." *Journal of Engineering Science and Technology*, vol. 7, pp. 916-934, 2016.

[24] G. Molau, "Heterogeneous ion-exchange membranes." *Journal of Membrane Science*, vol. 8, pp. 309-330, 1981.

[25] J. Fauvarque, S. Guinot, N. Bouzir, E. Salmon, J. Penneau, "Alkaline poly(ethylene oxide) solid polymer electrolytes. Application to nickel secondary batteries." *Electrochemica Acta*, vol. 40, pp. 2449-2453, 1995.

[26] E. Salmon, S. Guinot, M. Godet, J. Fauvarque, "Structural characterization of new poly (ethylene oxide) – based alkaline solid polymer electrolytes." *Journal of Applied Polymer Science*, vol. 3, pp. 601-607, 1997.

[27] L. Dragana, M. Ivana, M. Vladimir, L. Sladjana, P. Milica, "Enhanced performance of the solid alkaline fuel cell using PVA-KOH membrane." *International Journal of Electrochemical Science*, vol. 8, pp. 949-957, 2013.

[28] K. Uday, P. Hiralal, "Physically crosslinked KOH impregnated polyvinyl alcohol based alkaline membrane for direct methanol fuel cell." *The Canadian Journal of Chemical Engineering*, vol. 96, pp. 1888-1895, 2018.

[29] E. Antolini, E. Gonzalez, "Alkaline direct alcohol fuel cells." *Journal of Power Sources*, vol. 195, pp. 3431-3450, 2010.

[30] B. Xing, O. Savadogo, “Hydrogen/ oxygen polymer electrolyte membrane fuel cells ($PEMFC_s$) based on alkaline-doped polybenizimidazole (PBI).” *Electrochemistry Communications Journal*, vol. 2, pp. 697-702, 2000.

[31] Z. Hadis, J. Gaopeng, Y. Grace, F. Michael, C. Zhongwei, “High performance porous polybenzimidazole membrane for alkaline fuel cells.” *International Journal of Hydrogen Energy*, vol. 39, pp. 18405-18415, 2014.

[32] G. Wu, S. Lin, C. Yang, “Preparation and characterization of PVA/PAA membranes for solid polymer electrolytes.” *Journal of Membrane Science*, vol. 275, pp. 127-133, 2006.

[33] F. Jing, Q. Jinli, L. Rui, “Alkaline solid polymer electrolyte membranes based on structurally modified PVA/PVP with improved alkali stability.” *Polymer Journal*, vol. 51, pp. 4850-4859, 2018.

[34] M. Ünlü, J. Zhou, P. Kohl, “Hybrid anion and proton exchange membrane fuel cells.” *Journal of Phys. Chem.*, vol. 113, pp. 11416-11423, 2009.

[35] M. Aparicio, A. Jitianu, L. Klein, *Sol-gel processing for conventional and alternative energy*. New York: Springer, 2012, 399.

[36] X. Ying, L. Qing, M. Ai, M. Si, H. Qing, “Performance of organic-inorganic hybrid anion -exchange membranes for alkaline direct methanol fuel cells.” Journal of Power Sources, vol. 186, pp. 328-333, 2009.

[37] N. Liang, Y. Tu, D. Chen, H. Zhang, “Hybrid anio exchange membranes with self-assembled.” *Advance Polymer Technology Journal*, vol. 37, pp. 1732-1736, 2018.

[38] T. Feng, B. Lin, S. Zhang, N. Yuan, “Imidazolium-based organic-inorganic hybrid anion exchange membranes for fuel cell applications.” *Journal of Membrane Science*, vol. 508, pp. 7-14, 2018.

[39] Y. Zhu, C. Chen, D. Zuo, H. Zhang, “Hybrid anion-exchange membranes derived from quaternized polysulfone and functionalized titanium dioxide.” *Electrochemica Acta Journal*, vol. 177, pp. 128-136, 2015.

[40] Y. Ji, H. Kyu, R. Ae, J. Dong, “Graphene-mediated organic-inorganic composites with improved hydroxide conductivity and outstanding alkaline stability for anion exchange membranes.” *Composites Part B: Engineering-Journal*, vol. 164, pp. 324-332, 2019.

[41] Y. Wu, C. Wu, T. Xu, F. Yu, Y. Fu, “Novel anion-exchange organic-inorganic hybrid membranes: preparation and characterizations for potential use in fuel cells.” *Journal of Membrane Science*, vol. 321, pp. 299-308, 2008.

[42] X. Lin, C. Wu, Y. Wu, T. Xu, “Free-standing hybrid anion-exchange membranes for application in fuel cells.” *Journal of Applied Polymer Science*, vol. 126, pp. 3644-3651, 2012.

[43] L. Chikh, V. Delhorbe, O., Fichet, “Semi-Interpenetrating polymer networks as fuel cell membranes.” *Journal of Membrane Science*, vol. 368, pp. 1-17, 2011.

[44] X. Jiandang, L. Lei, L. Jiayou, S. Yinghua, L. Nanwen, “Semi-interpenetrating polymer networks by azide-alkyne cycloaddition as novel anion exchange membranes.” *Jouirnal of Materials Chemistry*, vol. 24, pp. 11317-11326, 2018.

[45] Y. Weihong, X. Peng, L. Xuezhuang, X. Yang, L. Yibin, Z. Baoliang, Z. Qiuyu, Y. Yi, "Mechanically robust semi-interpenetrating polymer network via thiol-ene chemistry for anion exchange membranes." *International Journal of Hydrogen Energy*, vol. 46, pp. 10377-10388, 2021.

[46] Z. Lingping, H. Oian, L. Yunchuan, K. Shangyi, "Anion exchange membrane based on interpenetrating polymer network with ultrahigh ion conductivity and excellent stability for alkalinne fuel cell." *Research Journal*, vol. 2020 pp. 1-11, 2020.

[47] L. Zeng, Y. Liao, J. Wang, Z. Wei, "Construction of highly efficient ion channel within anion exchange membrane based on interpenetrating polymer network for H_2/Air (CO_2-free) alkaline fuel cell." *Journal of Power Sources*, vol. 486, pp. 229377-229388, 2021.

[48] S. Sydonne, U. Nieves, T. María, V. Alejandro,. L. Belén, "Synthesis and characterization of novel anion exchange membranes based on semi-interpenetrating networks of functionalized polysulfone: effect of ionic crosslinking." *Polymers Journal*, vol. 13 pp. 958, 2021.

[49] W. Lu, Z. Shao, G. Zhang, J. Li, "Preparation of anion exchange membranes by an efficient chloromethylation method and homogeneous quaternization crosslinking strategy." *Journal of Solid State Ionics*, vol. 245-246, pp. 8-18, 2013.

[50] T. Sata, K. Teshima, T. Yamaguchi, "Permselectivity between two anions in anion exchange membranes crosslinked with various diamines in electrodialysis." *Journal of Polymer Science, Part A: Polymer Chemistry*, vol. 34, pp. 1475-1482, 1996.

[51] M. Iravaninia, S. Rowshanzamir, “Polysulfone-based anion exchange membranes for potential application in solid alkaline fuel cells.” *Journal of Renewable Energy and Environment*, vol. 2, pp. 59-65, 2015.

[52] M. Tomoi, T. Yamaguchi, R. Ando, Y. Kantake, Y. Aosaki, H Kubota, “Synthesis and thermal stability of novel anion exchange membrane resins with spacerchains.” *Journal of Applied Polymer Science*, vol. 64, pp. 1161-1167, 1997.

[53] Q. Ge, X. Zhu, Z. Yang, “Highly conductive and water-swelling resistant anion exchange mermbrane for alkaline fuel cells.” *International Journal of Molecular Sciences*, vol. 20, pp. 3470, 2019.

[54] K.Sayema, L. Asa, A. Ramez, T. Mengkun, A. Thomas, F. Tomoko, “Effect of morphology on anion conductive properties in self-assembled polystyrene-based copolymer membranes.” *Journal of Membrane Science*, vol. 565, pp. 213-225, 2018.

[55] H. Qing, L. Qing, B. Ian, M. Ai, X. Ying, P. Xing, “Anion exchange membranes based on quaternized polystyene-block-poly(ethylene-ran-butylene)-block-polystyrene for direct methanol alkaline fuel cells.” *Journal of Membrane Science*, vol. 349, pp. 237-243, 2010.

[56] K. Taro, M. Akinobu, I. Junji, M. Kenji, “Highly anion conductive polymers: how do hexafluoproisopropylidene groups affect membrane properties and alkaline fuel cell performance.” *Applied Energy Materials Journal*, vol. 1, pp. 469-477, 2020.

[57] Y. Luo, J. Guo, C. Wang, D. Chu, “Quaternized poly(methyl methacrylate-co-butyl acrylate-co-vinylbenzyl chloride) membrane for alkaline fuel cells.” *Journal of Power Sources*, vol. 195, pp. 3765-3771, 2010.

[58] D. Valade, F. Boshet, B. Améduri, “Synthesis annd modification of alternating copolymers based on vinyl ethers, chlorotrifluoroethylene, and hexafluoropropylene.” *Macromolecules Journal*, vol. 42, pp. 7689-7700, 2009.

[59] J. Varcoe, R. Slade, G. Wright, Y. Chen, “Steady-state dc and impedance investigations of H_2/O_2 alkaline membrane fuel cells with commercial Pt/C, Ag/C, and Au/C cathods.” *Journal of Physical Chemistry*, vol. 110, pp. 21041-21049, 2006.

[60] J. Varcoe, R. Slade, H. Lam, S. Poynton, D. Droscoll, D. Apperley, “Poly(ethylene-co-tetrafluoroethylene)-derived radiation-grafted anion-exchange membrane with properties specifically tailored for application in metal-cation-free alkaline polymer electrolyte fuel cells.” *Chemistry of Materials Journnal*, vol. 19, pp. 2686-2693, 2007.

[61] Y. Cao, X. Wang, M. Mamlouk, K. Scott, “Preparation of alkaline anion exchange polymer membrane from methylated melamine grafted poly (vinylbenzyl chloride) and its fuel cell performance.” *Journal of Materials Chemistry*, vol. 21, pp. 12910-12916, 2011.

[62] M. Schieda, S. Roualdès, J. Durand, A. Martinent, D. Marsac, “Plasma polymerized thin films as new membranes for miniature solid alkaline fuel cells.” *Desalination Journal*, vol. 199, pp. 286-288, 2006.

[63] K. Matsuoka, S. Chibaa, Y. Irioyama, T. Abe, M. Matsuoka, K. Kikuchi, Z. Ogumi, “Preparation of anion-exchange membrane by plasma polymerization and its use in alkaline fuel cells.” *Thin Solid Films Journal*, vol. 516, pp. 3309-3313, 2008.

[64] E. Dragan, E. Avran, D. Axente, C. Marcu, “Ion-exchange resins. lll. Functionalization-morphology correlations in the synthesis of some

macroporous, strong basic anion exchangers and uranium-sorption properties evaluation." *Journal of Polymer Science, Part A: Polymer Chemistry*, vol. 42 pp. 2451-2461, 2004.

[65] R. Vinodh, A. Ilakkiya, S. Elamathi, D. Sangeetha, "A novel anion exchange membrane from polystyrene (ethylene butylene) polystyrene: synthesis and characterization." *Materials Science and Engineering B: Solid-state Materials for Advanced Technology Journal*, vol. 167, pp. 43-50, 2010.

[66] Ă. Agel, J. Bouet, J. Fauvarque, H. Yassir, "The use of a solid polymer electrolyte in alkaline fuel cells." *Utilisation d´electrolyte solide polymere dans les piles a combustibles alcalines*, vol. 26, pp. 59-68, 2001.

[67] D. Stoica, F. Alloin, S. Marais, D. Langevin, C. Chappyey, S. Judein, "Polyepichlorohydrin membranes for alkaline fuel cells: sorption and conduction properties." *Journal of Physical Chemistry*, vol. 112, pp. 12338-12346, 2008.

[68] J. Hong, S. Hong, "Preparation of anion exchange membrane by amination of chlorinated polypropylene and ethylenediamine and its properties." *Journal of Applied Polymer Science*, vol. 115, pp. 2296-2301, 2010.

[69] Y. Xiong, J. Fang, Q. Zeng, Q. Liu, "Preparation and characterization of cross-linked quaternized poly(vinyl alcohol) membranes for anion exchange membrane fuel cells." *Journal of Membrane Science*, vol. 311, pp. 319-325, 2008.

[70] Y. Wan, B. Pepply, K. Creber, V. Bui, E. Halliop, "Quaternized-chitosan membranes for possible applications in alkaline fuel cells." *Journal of Power Source*, vol. 185, pp. 183-187, 2008.

[71] W. Lu, Z. Shao, G. Zhang, J. Li, Y. Zhao, B. Yi, “Preparation of anion exchange membranes by an efficient chloromethylation method and homogeneous quaternization/ crosslinking strategy.” *Solid State Ionics Journal*, vol. 245-246, pp. 8-18, 2013.

[72] M. Iravaninia, S. Azizi, S. Rowshanzamir, “Investigation of ion transport and water content properties in anion exchange membranes based on polysulfone for solid alkaline fuel cell application.” *Iranian Journal of Hydrogen & Fuel Cell*, vol. 1, pp. 13-25, 2015.

[73] K. Gopi, S. Peera, S. Bhat, P. Sridhar, S. Pitchumani, “3-Methyltrimethylammonium poly(2,6-dimethyl-1,4-phenylene oxide) based anion exchange membrane for alkaline polymer electrolyte fuel cells.” *Bull Material Science*, vol. 37, pp. 877-881, 2014.

[74] X. Zijun, Y. Sen, “Polybenzimidazoles with pendant quaternary ammonium groups as potential anion exchange membranes for fuel cells.” *Journal of Membrane Science*, vol. 390-391, pp. 152-159, 2012.

[75] H. Zarrin, J. Wu, M. Fowler, Z. Chen, “High durable PEK-based anion exchange membrane for elevated temperature alkaline fuel cells.” *Journal of Membrane Science*, vol. 394-395, pp. 193-201, 2012.

[76] M. Iravaninia, S. Rowshanzamir, “Polysulfone-based anion exchange membranes for potential application in solid alkaline fuel cells.” *Journal of Renewable Energy and environment*, vol. 2, pp. 59-65, 2015.

[77] R. Varcoe, A. Plamen, “Anion-exchange membranes in electrochemical energy systems.” *Energy Environ Science*, vol. 7, pp. 3135-3191, 2014.

[78] G. Xi, Y. Chun, “Synthesis and characterization of qwuaternized poly(phthalazinone ether sulfone ketone) for anion exchange membrane.” *Chinese Chemical Letters*, vol. 18, pp. 1269-1272, 2007.

[79] W. Liang, X. Tongwen, W. Dan, Z. Xin, “Preparationm and characterization of CPPO/ BPPO blend membranes fpr potential application in alkaline direct methanol fuel cell.” *Journal of Membrane Science*, vol. 310, pp. 577-585, 2008.

[80] R. Hamid, M. Mahdieh, G. Mehdi, “Synthesis of porous polyether sulfone ion-exchange membrane, investigation on its properties and characterizations,” presented at The 8th Int. Chemical Engineering Congress & Exhibition, Kish, Iran, 2014.